



Surrogate-assisted evolutionary algorithm with hierarchical surrogate technique and adaptive infill strategy

Hao Chen^{a,b,c}, Weikun Li^{c,b}, Weicheng Cui^{b,c,*}

^a Zhejiang University-Westlake University Joint Training, Zhejiang University, Hangzhou 310024, Zhejiang Province, China

^b Key Laboratory of Coastal Environment and Resources of Zhejiang Province, School of Engineering, Westlake University, 18 Shilongshan Road, Hangzhou 310024, Zhejiang Province, China

^c Institute of Advanced Technology, Westlake Institute for Advanced Study, 18 Shilongshan Road, Hangzhou 310024, Zhejiang Province, China

ARTICLE INFO

Keywords:

Surrogate-assisted optimization
High-dimensional model representation
Infill sampling strategy
Surrogate modeling

ABSTRACT

Fitness functions of real-world optimization problems often need to be analyzed by expensive experiments or numerical simulations. Integrating these expensive simulations or experiments directly into optimization algorithms would result in substantial computational costs. Surrogate-assisted evolutionary algorithms (SAEAs) have attracted massive attention recently due to their high efficiency and applicability in solving real-world optimization problems. As the dimension of the optimization problem increases, the computational cost of constructing surrogates increases, and the surrogate model's prediction accuracy may be severely degraded. High-dimensional model representation (HDMR) is a promising technique to partition a high-dimensional function into low-dimensional component functions. However, HDMR's hierarchical structure limits its applicability in online SAEAs. To address these problems, this paper develops a surrogate-assisted evolutionary algorithm with hierarchical surrogate technique and adaptive infill strategy (SAEA-HAS). In this work, we propose a novel hierarchical surrogate technique, in which a composite surrogate model is constructed by the first-order HDMR model and an error value-based surrogate model, then, using the internal contrastive analysis method, a hierarchical surrogate model (HSM) combining the composite surrogate with the fitness value-based surrogate is established. In addition, an adaptive infill strategy is developed to balance the exploration and exploitation of the surrogate-assisted evolutionary search. Various test functions and an antenna optimization problem are employed to compare SAEA-HAS with several well-known SAEAs. The experimental results validate the effectiveness of SAEA-HAS.

1. Introduction

Evolutionary algorithms (EAs) have been widely applied in solving real-world optimization problems (Bi, Xue, & Zhang, 2021; Chen, Li, Cui, et al., 2020; Gao, Wang, Yu, & Yue, 2022; Hong, Cui, & Chen, 2021; Lan et al., 2022). Traditional EAs are developed on the assumption that the objective function is explicit and the fitness evaluations (FEs) are cheap (Li, Zhan & Zhang, 2022a). However, objective functions of many real-world optimization problems are usually implicit and the fitness evaluations are based on high-fidelity numerical simulations or physical experiments (Li, Chen, Cui, Song & Chen, 2022; Liu, Liu, & Jin, 2022). Thus, traditional EAs cannot handle real-world optimization problems. Surrogate-assisted evolutionary optimization algorithms (SAEAs) employ a certain amount of FEs and computationally cheap surrogate models to drive EAs, which has been shown to be effective in solving implicit and expensive real-world optimization problems (Jin,

Wang, Chugh, Guo, & Miettinen, 2019; Li, Zhan, Wang & Zhang, 2020; Wang, Feng, Jin, & Doherty, 2021; Wu, Yu, & Liang, 2023). Depending on whether additional real FEs can be obtained during optimization, the existing SAEA algorithms can be classified into two categories: offline SAEAs and online SAEAs. Offline SAEAs are developed on the assumption that no additional real FEs can be obtained during optimization (Huang & Wang, 2021). Because only the historical data set is available or the computational cost of simulation is too high, in some complex real-world offline optimization problems, including the trauma system design problem (Wang, Jin, & Jansen, 2016), the magnesium furnace optimization problem (Guo, Chai, Ding, & Jin, 2016), the blast furnace design optimization problem (Chugh, Chakraborti, Sindhya, & Jin, 2017), the airfoil shape optimization problem (Andrés-Pérez et al., 2019) and the underwater robot design problem (Chen, Li, Cui, Yang, & Chen, 2021), no additional real FEs can be provided.

* Corresponding author at: Key Laboratory of Coastal Environment and Resources of Zhejiang Province, School of Engineering, Westlake University, 18 Shilongshan Road, Hangzhou 310024, Zhejiang Province, China.

E-mail addresses: chenhao@westlake.edu.cn (H. Chen), liweikun@westlake.edu.cn (W. Li), cuiweicheng@westlake.edu.cn (W. Cui).

<https://doi.org/10.1016/j.eswa.2023.120826>

Received 1 January 2023; Received in revised form 28 May 2023; Accepted 10 June 2023

Available online 16 June 2023

0957-4174/© 2023 Published by Elsevier Ltd.

Offline SAEAs cannot add new sample points during optimization to improve the model accuracy, which makes offline SAEAs more complicated than online SAEAs. On the contrary, online SAEAs are based on the assumption that the real fitness values of a certain amount of new samples can be evaluated during optimization (Cui, Li, Zhou, & Abusorrah, 2022; Zhen, Gong, Wang, Ming, & Liao, 2021; Zhou, Ong, Nguyen, & Lim, 2005).

Surrogate models are undoubtedly a key research direction in SAEAs. Most parts of SAEAs, including model construction, fitness evaluation and model updating, are related to surrogate models (Tong, Huang, Minku, & Yao, 2021). Many surrogate models such as Response Surface Method (Box, Hunter, Hunter, et al., 1978), Radial Basis Function (Hardy, 1971), Kriging (Sacks, Welch, Mitchell, & Wynn, 1989), Multivariate Adaptive Regression Splines (Friedman, 1991), Support Vector Regression (Cristianini, Shawe-Taylor, et al., 2000) and Artificial Neural Network (Hassoun et al., 1995; Vt & Shin, 1994) can be used in SAEAs. In addition to those stand-alone surrogate models, many ensembles of surrogates have been proposed to improve the surrogate robustness and accuracy (Goel, Haftka, Shyy, & Queipo, 2007). Due to the high robustness, ensembles of surrogates are widely used to build the global surrogate in SAEAs. Combining various ensembles of surrogates with adaptive surrogate selection criteria, Yu, Li, and Liang (2020) developed an adaptive surrogate model-based evolutionary algorithm. As the dimension increases, the model construction cost of ensembles of surrogates increases dramatically, which will decrease the efficiency of the SAEA framework (Chen, Li, Cui, & Liu, 2022). High-dimensional model representation (HDMR) (Shan & Wang, 2010) is a promising technique to partition a high-dimensional function into low-dimensional component functions. Various HDMRs models such as analysis of variance-based HDMR (ANOVA-HDMR) (Rabitz & Aliş, 1999), cut point-based HDMR (cut-HDMR) (Rabitz, Aliş, Shorter, & Shim, 1999) and random sampling HDMR (RS-HDMR) (Li et al., 2006) have been proposed in terms of the choice of different projection operators. The cut-HDMR technique has been widely combined with surrogate models for function approximation and global optimization due to its advantages of easy construction and high precision (Jiang, Yang, Wang, Miao, & Bai, 2021; Li & Wang, 2016; Li, Wang, & Ye, 2016; Liu, Hervas, Ong, Cai, & Wang, 2018; Mukhopadhyay, Dey, Chowdhury, Chakrabarti, & Adhikari, 2015; Wu, Peng, Chen, & Zhang, 2019; Zhang, Wang, Dong, & Li, 2020). Many surrogate models can be employed to approximate component functions in the cut-HDMR expansion (Yue, Zhang, Gong, Luo, & Duan, 2021). However, cut-HDMR's hierarchical structure limits its applicability in online surrogate-assisted evolutionary optimization (Cai, Gao, & Li, 2019) because the construction of the cut-HDMR model requires the structured sampling method such as the dividing rectangles (DIRECT) sampling method (Chen, Wang, Ye, & Hu, 2019), in which the training points are sampled in a specific way. Therefore, once the cut-HDMR-based surrogate model is constructed, the newly filled sample points cannot be used to directly update the cut-HDMR-based surrogate model. All the above surrogate techniques are regression-based models that directly model the relationship between design variables and the fitness function. In recent years, some classification-based surrogate models are developed (Lu, Tang, & Yao, 2011; Ziegler & Banzhaf, 2003). Different from regression-based surrogate models, classification-based surrogate models only use the comparison results between individuals and the reference point. Lu et al. (2011) developed a classification-based SAEA framework for solving single-objective optimization problems using a differential evolution algorithm, in which the soft-margin support vector classification (Chen, Wu, Ying, & Zhou, 2004) is adopted as the classifier. The parent is chosen as the current generation's reference solution for each offspring.

In addition to the surrogate model, the core research contents of offline SAEAs include two aspects. The first is to improve the amount of available offline data to improve the model accuracy, especially when the offline data set is small. In general, the more offline data,

the better the prediction performance of the surrogate model can be achieved (Wang, Jin, Sun, & Doherty, 2018). Some methods of increasing the amount of offline data have been proposed in recent years, such as artificial data generation (Farzaneh & Mahdian Toroghi, 2019) and localized data generation (Li, Zhan, Wang, Jin & Zhang, 2020). The other research content is to develop effective offline surrogate model management strategies (Huang, Wang, & Jin, 2021; Huang, Wang, & Ma, 2019; Wang et al., 2018; Zhen, Gong, & Wang, 2022) to guide the evolutionary search. For online SAEAs, except those research focuses included in offline SAEAs, how to select the most potential candidate solution during optimization and update the surrogate with its true fitness value (Known as infill sampling criteria (Li, Gao, Garg, Shen, & Huang, 2021a)) is also a key research content of online SAEAs. In general, there are two types of infill criteria, the performance-based infill strategy and the uncertainty-based infill strategy. The performance-based criteria (Jin, Olhofer, Sendhoff, et al., 2000) evaluates the actual objective values of individuals with the minimum predicted value in the population, which can enhance the exploitation performance of surrogates in the promising area. However, previous research has shown that the performance-based infill strategy may cause the SAEA to converge prematurely (Razavi, Tolson, & Burn, 2012). Since Kriging model can give the prediction variance, various Kriging-based uncertainty infill strategies have been developed in online SAEAs to balance the exploration and exploitation during optimization, including the probability of improvement (PoI) (Zhou, Ong, Nair, Keane, & Lum, 2006), expected improvement (ExI) (Emmerich, Giannakoglou, & Naujoks, 2006) and lower confidence bound (LCB) (Liu, Grout, & Nikolaeva, 2017). In addition to the Kriging model, the minimum distance to training samples (Li, Zhang, Sun & Han, 2019), and the discrepancy of predictions from the ensemble of surrogates (Li, Cai & Gao, 2019) can also be employed to provide the uncertainty information.

Many recent studies have focused on combining accurate surrogate models with efficient infill sampling strategies to assist EAs. Wang, Jin, and Doherty (2017) developed a committee-based active learning method for surrogate-assisted particle swarm optimization, in which the uncertainty-based and performance-based infill strategies are used simultaneously. Both two strategies are based on the ensemble of surrogates to search for the solution with the maximum uncertainty and the best solution with the minimum predicted fitness value. Fu, Sun, Tan, Zhang, and Jin (2020) developed a surrogate-assisted evolutionary optimization algorithm using a random feature selection approach (SAEA-RFS), in which the optimization problem is optimized by sequentially optimizing several sub-problems that are formed with the random feature selection. Li, Gao, Garg, Shen, and Huang (2021) collaboratively used convergence-based and diversity-based strategies to select promising solutions for real fitness evaluations. Liu, Wu, Lin, Ji, and Wong (2021) proposed an efficient SAEA with an uncertainty grouping-based infill sampling criteria (SAEA-UGC), in which the prediction difference among surrogates is adopted as the uncertainty information to select the promising solution. Then the updated ensemble of surrogates is applied for global search and a reconstructed RBF model is responsible for the local search. Yu, Liang, Wu and Yang (2022) developed a heterogeneous ensemble surrogate-driven neighborhood field optimizer (HESNFO), in which both the accuracy and diversity of surrogate models are considered to speed up the convergence process. A two-fold infill sampling strategy is proposed to balance the exploration and exploitation of HESNFO. Combining a Lipschitz-based surrogate with a differential evolution-based optimizer, Kudela and Matousek (2023) proposed a novel Lipschitz surrogate model-assisted differential evolution algorithm (LSADE). Yu, Liang, Zhao and Wu (2022) presented a novel adaptive surrogate model management strategy using multiple RBF parallel modeling method for online SAEA (aRBF-NFO).

In this work, a surrogate-assisted evolutionary algorithm with hierarchical surrogate technique and adaptive infill strategy (SAEA-HAS) is developed. The proposal of hierarchical surrogate technique is based on the following two motivations. First, although many valuable surrogate

models in machine learning have been used in SAEAs, the prediction accuracy of these surrogates decrease dramatically when the dimension increases, which will decrease the convergence of SAEAs. HDMR is a promising technique to partition a high-dimensional function into low-dimensional component functions, this technique has been widely used in function approximation due to its advantages of easy construction and high precision. Second, HDMR's hierarchical structure limits its applicability in online SAEA, because the construction of the HDMR model requires the structured sampling method. The newly filled sample points cannot be used to directly update the HDMR-based surrogate model. Therefore, to inherit the advantages of HDMR model and bridge the gap between HDMR and online SAEAs, this paper presents for the first time the error value-based surrogate to characterize the error relationship between the HDMR-based surrogate and the real fitness function, it can be updated using newly filled samples during optimization. As a result, by combining first-order HDMR model and the error value-based surrogate model, the proposed composite surrogate model can be integrated into online SAEAs. Thus breaking the barrier between the HDMR-based surrogate modeling and online SAEAs.

The training database in SAEA-HAS is divided into two data subsets. The first training subset is generated by the structured sampling method for building the first-order cut-HDMR-based surrogate model. The second training subset is employed to perform the contrastive analysis. The prediction accuracy of cut-HDMR-based surrogate models is unsatisfactory when approximating functions with a large number of high-order interactions between input variables. Therefore, an internal contrastive analysis method is proposed to establish the hierarchical surrogate model (HSM) by combining the composite surrogate with the fitness value-based surrogate, which can enhance the robustness of the SAEA-HAS for different optimization problems. The radial basis function (RBF) model (Hardy, 1971) widely used in SAEAs is employed in this paper to build the first-order cut-HDMR model and the error value-based surrogate due to its high accuracy and efficiency. Then an adaptive infill strategy is proposed to update the HSM during optimization and balance the exploration and exploitation of the surrogate-assisted evolutionary search. In the adaptive infill strategy, the individual with the minimum predicted value in each iteration is evaluated using the real fitness function to help the surrogate refine the current promising area. Then a mutation operator is designed to assist the exploration and exploitation of the proposed SAEA. The designed mutation operator is applied to the best individual to generate a new individual. The two new individuals evaluated by the real fitness function are used to update the HSM. The cut-HDMR-based surrogate model can be efficiently integrated into online SAEAs for optimization using the hierarchical surrogate technique and the adaptive infill strategy.

The main contributions of this paper are highlighted as follows.

- A novel hierarchical surrogate technique is proposed, in which a composite surrogate model is constructed by the first-order HDMR model and an error value-based surrogate model. Then, using the internal contrastive analysis method, a hierarchical surrogate model is established by combining the composite surrogate with the fitness value-based surrogate. The infill points generated during optimization in SAEA can be used to update the HSM, breaking the barrier between the cut-HDMR-based surrogate modeling and online SAEAs.
- An adaptive infill strategy is developed to update the hierarchical surrogate model and enhance the exploration and exploitation abilities of the surrogate-assisted evolutionary search.

The remainder of this paper is organized as follows, the prior knowledge related to the HDMR and RBF models is introduced in Section 2. Details of the proposed SAEA-HAS are presented in Section 3. Section 4 gives the experimental setting and results analysis of test functions and an antenna optimization problem. Finally, Section 5 gives the concluding remarks.

2. Related work

2.1. High-dimensional model representation (HDMR)

In HDMR, a hierarchical function expansion according to design variables is employed to estimate the fitness function:

$$f(x) = f_0 + \sum_{i=1}^D f_i(x_i) + \sum_{1 \leq i < j \leq D} f_{ij}(x_i, x_j) + \sum_{1 \leq i < j < k \leq D} f_{ijk}(x_i, x_j, x_k) + \dots + f_{12\dots D}(x_1, x_2, \dots, x_D) \quad (1)$$

Where f_0 represents the zero-order component function, indicating the mean value of $f(x)$ over the design domain. The first-order function $f_i(x_i)$ represents the contribution of design variable x_i to the output $f(x)$. $f_{ij}(x_i, x_j)$ is the second-order term, indicating the cooperative contribution of design variables x_i, x_j to $f(x)$. The high-order component functions denote the interacting effects of an increasing number of design variables to $f(x)$. $f_{12\dots D}(x_1, x_2, \dots, x_D)$ reflects any residual interacting effects of all design variables to $f(x)$. To reduce computational cost and keep the tolerable prediction accuracy, the expansion of HDMR to the second order is generally considered sufficient to represent the output (Shan & Wang, 2010).

$$f(x) \approx f_0 + \sum_{i=1}^D f_i(x_i) + \sum_{1 \leq i < j \leq D} f_{ij}(x_i, x_j) \quad (2)$$

The expansion of cut-HDMR is an exact representation of the response $f(x)$, so the underlying problem can be transformed into an explicit function of low-order correlations. This approach is independent of the choice of the cut point x_c , which is usually chosen within the domain of interest in the input space. The structure of each component function in cut-HDMR expansion is as follows:

$$f_0 = f(x_c) \quad (3)$$

$$f_i(x_i) = f(x_i, x_c^i) - f_0 \quad (4)$$

$$f_{ij}(x_i, x_j) = f(x_i, x_j, x_c^{ij}) - f_i(x_i) - f_j(x_j) - f_0 \quad (5)$$

Where x_c represents the cut point that is usually selected at the center of design space, f_0 is the real fitness value of x_c . x_c^i represents the cut point without the i th dimension, and x_c^{ij} indicates the cut point without dimensions i, j . The first-order function $f_i(x_i)$ is calculated along its i th design variable axis (i.e., the i th, cut line) through the cut point. The second-order term is calculated in a plane defined by the design variables x_i, x_j . The cut-HDMR ignores higher-order terms, assuming that after accounting for the effects of individual input variables and their lower-order correlations, the effects of higher-order correlations are small (Liu et al., 2018).

2.2. Radial basis function model (RBF)

The RBF model is widely used in SAEAs due to its high accuracy and efficiency. RBF model is especially suitable for problems with high dimensions because the modeling time of the RBF model increases insignificantly with the dimension. Assume that the training data set $\{(x_i, y_i) | i = 1, 2, \dots, H\}$ is constructed by H samples with D dimension, the expression of RBF model is shown below:

$$\hat{f}(x) = \sum_{j=1}^H w_j \phi(\|x - x_j\|) \quad (6)$$

Where $\phi(\cdot)$ denotes the kernel function, $\|\cdot\|$ refers to the Euclidian norm and w_j is the weight of the j th kernel function. The Gaussian kernel function expressed in Eq. (7) is employed in this work.

$$\phi(x) = \exp\left(\frac{-x^2}{2\delta^2}\right) \quad (7)$$

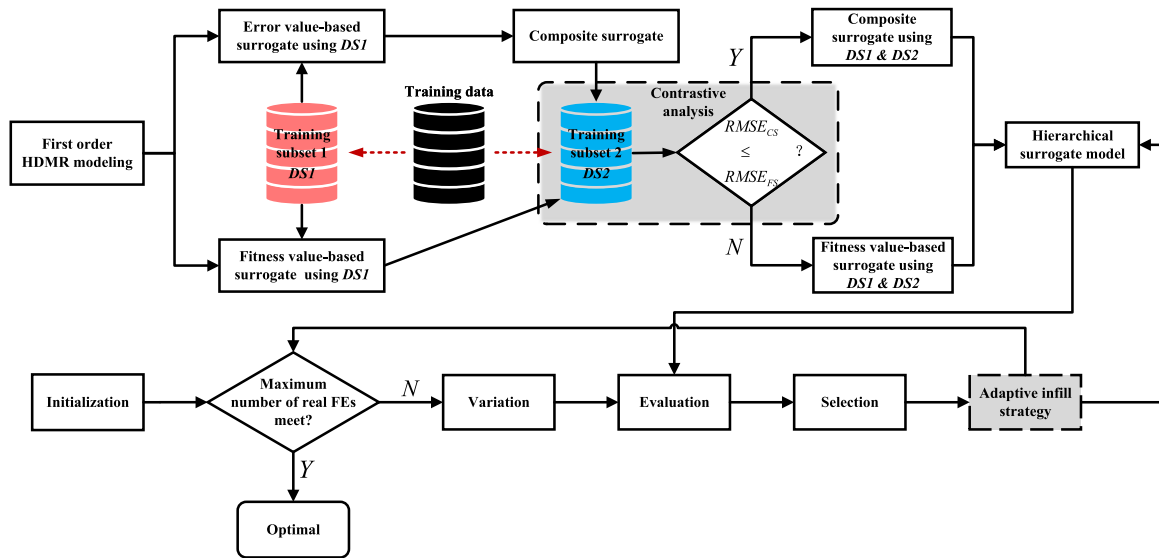


Fig. 1. Diagram of the SAEA-HAS.

Where δ refers to the Gaussian function's hyper-parameter. The RBF model can be built quickly when the training data and the hyper-parameter are given. The weight w is calculated as follows:

$$w = \left[\phi(\|x_i - x_j\|) \right]_{H \times H}^{-1} F \quad (i, j = 1, 2, \dots, H) \quad (8)$$

Where $F = [f_1, f_2, \dots, f_H]^T$ is the real fitness vector of the training set, $\left[\phi(\|x_i - x_j\|) \right]_{H \times H}$ represents kernel matrix of the training data set.

3. Proposed SAEA-HAS algorithm

3.1. Framework of SAEA-HAS

The diagram of SAEA-HAS is depicted in Fig. 1, the training database consists of two data subsets. The first training subset DS_1 is generated by the modified DIRECT sampling method, which is used to construct the first order RBF-HDMR model. Then DS_1 is employed to build the error value-based RBF model, which is used to characterize the error relationship between the first-order RBF-HDMR and the real fitness function. Then a composite surrogate model is built by combining the first-order RBF-HDMR and the error value-based RBF model. The prediction accuracy of cut-HDMR-based surrogate models is unsatisfactory when real fitness functions include many high-order interactions between input variables. Therefore, an internal contrastive analysis method is proposed to establish the HSM by combining the composite surrogate with the fitness value-based RBF model, which can enhance the robustness of the SAEA-HAS for different optimization problems. The second training subset DS_2 is generated by the Latin Hypercube Sampling (LHS) technology (Loh, 1996). DS_2 is employed to perform the contrastive analysis.

After the HSM is determined, the database is updated with the two training data subsets DS_1 and DS_2 . Find the best individual in the database, and set it to the current best individual. A generic genetic algorithm (GA) is adopted as the optimization algorithm. Simulated binary crossover (SBX) and polynomial mutation are used to produce offspring. The HSM is used to predict the fitness values in the current population; the N_p individuals with smaller predicted fitness values are selected to update the population. Then the adaptive infill strategy is employed to add new points to enhance the exploration and exploitation abilities of the surrogate-assisted evolutionary search and refine the HSM. Finally, the HSM is updated with the infill points for the next iteration. If the composite surrogate is selected in the HSM, the infill points are used to update the error value-based RBF

surrogate. When the number of extra real fitness evaluations reaches the maximum number, the proposed SAEA-HAS will output the optimal solution. The pseudo-code of the overall framework of SAEA-HAS is shown in Algorithm 1.

Algorithm 1 The framework of SAEA-HAS.

Input: Size of training set 2 N_{s2} , Population size N_p , Dimension of design space D , Upper and Lower bounds of design space X_U, X_L , Maximum number of extra fitness evaluations N_{mf} , Crossover and Mutation probabilities p_c, p_m , Cut point x_c , Sampling factor β , Convergence criteria ϵ_1 , Real fitness function f , Parameter vector of RBF model η .

- 1: First-order RBF-HDMR modeling ($x_c, \beta, \epsilon_1, f, \eta, X_U, X_L, D$). [Refer to algorithm 2].
- 2: Obtain first-order RBF-HDMR model $\hat{f}^1(x)$ and training data set 1 DS_1 .
- 3: Hierarchical surrogate modeling ($N_{s2}, DS_1, DS_2, \eta, \hat{f}^1(x), X_U, X_L, D$). [Refer to algorithm 3].
- 4: Obtain hierarchical surrogate model $\hat{f}(x)$.
- 5: Initialize the database $DB = [DS_1; DS_2]$.
- 6: Find the best individual x_{db1} in the DB . The current best individual $x_b = x_{db1}$.
- 7: $cFEs = 0$.
- 8: **while** $cFEs < N_{mf}$ **do**
- 9: Generate the offspring Pop_s . $Pop = [Pop; Pop_s]$.
- 10: Estimate fitness values of the Pop using $\hat{f}(x)$.
- 11: Sort the Pop in terms of the estimated fitness values and select the best N_p individuals. The best N_p individuals are used to update Pop such that Pop remains a fixed number during iterations.
- 12: Adaptive infill strategy ($Pop(1), DB, D, cFEs, N_{mf}$). [Refer to algorithm 4].
- 13: Update $\hat{f}(x)$ with the infill points.
- 14: **end while**

Output: The optimal solution.

3.2. First-order RBF-HDMR modeling

The first-order RBF-HDMR meta-modeling technique attempts to use RBF to construct a cut-HDMR model based on the modified DIRECT sampling method (Yue et al., 2021). The main sampling criteria of the modified DIRECT sampling method are as follows. First, the initial sample points are set at each variable range's upper and lower limits,

Algorithm 2 First-order RBF-HDMR modeling.

Input: $x_c, \beta, \varepsilon_1, f, \eta, X_U, X_L, D$.

- 1: Evaluate the fitness of x_c as f_0 .
- 2: **for** $i = 1 : D$ **do**
- 3: Add two end points $(x_i^-, x_c^l), (x_i^+, x_c^l)$ along the i th cut line and evaluate their first-order fitness values $f_i(x_i^-) = f(x_i^-, x_c^l) - f_0, f_i(x_i^+) = f(x_i^+, x_c^l) - f_0$.
- 4: Add $(x_i^-, x_c^l), (x_i^+, x_c^l)$ to the first-order training set $\{X_i^1, Y_i^1\}$ and construct the i th first-order RBF model $\hat{f}_i(x_i) \leftarrow \{X_i^1, Y_i^1\}$.
- 5: Randomly generate a sample point (x_i^r, x_c^l) along i th cut line and evaluate the $f_i(x_i^r) = f(x_i^r, x_c^l) - f_0$.
- 6: Evaluate cr_1, cr_2, cr_3 by Eqs. (9–11). Add $(x_i^r, f_i(x_i^r))$ to $\{X_i^1, Y_i^1\}$, construct $\hat{f}_i(x_i) \leftarrow \{X_i^1, Y_i^1\}, flag = 0$.
- 7: **if** $cr_1 > \varepsilon_1 \cup cr_2 > \varepsilon_1 \cup cr_3 > \varepsilon_1$ **then**
- 8: **while** $flag \neq 1$ **do**
- 9: Determine the optimal interval of the i th cut line ivf_i by Eq. (12).
- 10: Sample a new point x_i^w according to Eq. (13).
- 11: Calculate Δ_x by Eq. (14).
- 12: **if** $\Delta_x < 0.1$ **then**
- 13: Determine the optimal interval of the i th cut line ivp_i by Eq. (15).
- 14: Sample a new point x_i^s by Eq. (16).
- 15: **if** $ivf_i = ivp_i$ **then**
- 16: Add $(x_i^s, f_i(x_i^s))$ to $\{X_i^1, Y_i^1\}$. Reconstruct $\hat{f}_i(x_i) \leftarrow \{X_i^1, Y_i^1\}$.
- 17: Calculate cr_4 of x_i^s by Eq. (17).
- 18: **if** $cr_4 \leq \varepsilon_1$ **then**
- 19: $flag = 1$.
- 20: **end if**
- 21: **else**
- 22: $flag = 1$.
- 23: **end if**
- 24: **else**
- 25: Calculate cr_4 of x_i^w by Eq. (17).
- 26: **if** $cr_4 \leq \varepsilon_1$ **then**
- 27: Determine the optimal interval of the i th cut line ivp_i by Eq. (15).
- 28: Sample a new point x_i^q according to Eq. (16).
- 29: **if** $ivf_i = ivp_i$ **then**
- 30: $flag = 1$.
- 31: **else**
- 32: Calculate cr_4 of x_i^q by Eq. (17).
- 33: **if** $cr_4 \leq \varepsilon_1$ **then**
- 34: $flag = 1$.
- 35: **end if**
- 36: Add $(x_i^q, f_i(x_i^q))$ to $\{X_i^1, Y_i^1\}$.
- 37: **end if**
- 38: **end if**
- 39: Add $(x_i^w, f_i(x_i^w))$ to $\{X_i^1, Y_i^1\}, \hat{f}_i(x_i) \leftarrow \{X_i^1, Y_i^1\}$.
- 40: **end if**
- 41: **end while**
- 42: **end if**
- 43: **end for**

Output: First-order RBF-HDMR $\hat{f}^1(x) = f_0 + \sum_{i=1}^D \hat{f}_i(x_i)$, Training data set $1 DS_1$.

and the RBF model is constructed. Then the DIRECT algorithm is used to evaluate the response of the sample points generated based on the maximum response difference or the maximum interval difference in the potential rectangle. Take more samples around highly non-linear regions by setting the underlying rectangle of DIRECT at the current sample with the largest prediction difference. The pseudo-code of the

first-order RBF-HDMR modeling is shown in Algorithm 2. The modeling process consists of the following steps:

Step1. Initialize the first-order RBF model. At first, choose the center of the input space as the cut point x_c , and calculate the response f_0 . Sample two points along the i th cut line (i.e., i th dimension of the cut point) at the lower and upper bounds of the cut point $(x_i^-, x_c^l), (x_i^+, x_c^l)$, respectively. Evaluate their first-order fitness values, $f_i(x_i^-), f_i(x_i^+)$ and construct the i th first-order RBF model. Randomly generate a sample point (x_i^r, x_c^l) along i th cut line and evaluate the first-order fitness value $f_i(x_i^r)$. Calculate the three convergence metrics cr_1, cr_2, cr_3 using Eqs. (9)–(11). Add $(x_i^r, f_i(x_i^r))$ to the i th first-order training set $\{X_i^1, Y_i^1\}$, construct $\hat{f}_i(x_i)$ using $\{X_i^1, Y_i^1\}$.

$$cr_1 = \left| \frac{\hat{f}_i(x_i^r) - f_i(x_i^r)}{f_i(x_i^r)} \right| \tag{9}$$

$$cr_2 = \left| \frac{\hat{f}_i(x_i^r)}{f_0} \right| \tag{10}$$

$$cr_3 = \left| \frac{f_i(x_i^+) - \hat{f}_i(x_i^c) - \hat{f}_i(x_i^c) - f_i(x_i^-)}{x_i^+ - x_i^-} \right| \tag{11}$$

Step2. Check the linearity of the first-order RBF model. If all convergence metrics satisfy the demand for precision, the first-order RBF model is considered linear. Finish the i th first-order RBF-HDMR modeling.

Otherwise, when the cyclic condition is satisfied, determine the optimal interval of the i th cut line ivf_i by the following equation.

$$ivf_i = \max(|f_i(x_i^{e+}) - f_i(x_i^{e-})|) \tag{12}$$

Where x_i^{e+} and x_i^{e-} represent the positions of the upper and lower endpoints of each interval on the i th cut line, respectively. Then, sample a new point according to the following equation:

$$x_i^w = \frac{x_i^{f<} + (1 + \beta)x_i^{f>}}{2 + \beta} \tag{13}$$

Where $x_i^{f<}$ represents the endpoint with a smaller response value in the optimal interval based on the maximum response difference and $x_i^{f>}$ is the endpoint with a larger response value in the optimal interval. β indicates the sampling factor. Calculate the boundary metric using the following equation:

$$\Delta_x = \left\| x_i^{f>} - x_i^{f<} \right\|_2 \tag{14}$$

Step3. First-order RBF-HDMR modeling when the optimal interval length based on the maximum response difference satisfies the convergence criteria.

If Δ_x satisfies the convergence criteria, determine the optimal interval of the i th cut line ivp_i based on the maximum length difference by the following equation:

$$ivp_i = \max(|x_i^{e+} - x_i^{e-}|) \tag{15}$$

Sample a new point according to the following equation:

$$x_i^s = \frac{x_i^{p<} + (1 + \beta)x_i^{p>}}{2 + \beta} \tag{16}$$

Where $x_i^{p<}$ represents the endpoint with a smaller response value in the optimal interval based on the maximum length difference and $x_i^{p>}$ is the endpoint with a larger response value in the optimal interval. If $ivf_i = ivp_i$, set the cycling condition to false. Otherwise, add $(x_i^s, f_i(x_i^s))$ to $\{X_i^1, Y_i^1\}$. Reconstruct $\hat{f}_i(x_i)$ using $\{X_i^1, Y_i^1\}$. Calculate convergence criteria cr_4 of x_i^s by Eq. (17). If cr_4 meets the convergence criteria, set the cycling condition to false.

$$cr_4 = \left| \frac{\hat{f}_i(x_i^{new}) - f_i(x_i^{new})}{f_i(x_i^{new})} \right| \tag{17}$$

Step4. First-order RBF-HDMR modeling when the optimal interval length based on the maximum response difference does not satisfy the convergence criteria.

If Δ_x does not meet the criteria, calculate convergence criteria cr_4 of x_i^w by Eq. (17). When cr_4 meets the convergence criteria, determine the optimal interval of the i th cut line ivp_i by Eq. (15). Sample a new point x_i^q according to Eq. (16). If $ivf_i = ivp_i$, set the cycling condition to false. Otherwise, calculate convergence criteria cr_4 of x_i^q by Eq. (17). If cr_4 of x_i^q meets the convergence criteria, set the cycling condition to false. Add $(x_i^q, f_i(x_i^q))$ to $\{X_i^1, Y_i^1\}$, set the cycling condition to false.

Add $(x_i^w, f_i(x_i^w))$ to $\{X_i^1, Y_i^1\}$. Repeat steps 1 to 4 until all first-order component functions are constructed. So far, the construction of the first-order RBF-HDMR model is completed.

3.3. Hierarchical surrogate technique

The hierarchical surrogate technique shown in algorithm 3 consists of three steps. Firstly, the fitness and error value-based RBF models are constructed using the training data subset 1. Secondly, the composite surrogate model CS is built by combining the first-order RBF-HDMR model and the error value-based RBF model. Then the comparison of CS and the fitness value-based RBF model are conducted through the contrastive analysis, in which the $RMSE$ values of these two surrogates on the training data subset 2 are calculated, the surrogate with the smaller $RMSE$ value is selected as the HSM. Finally, the chosen surrogate is constructed on the database.

Algorithm 3 Hierarchical surrogate modeling.

Input: $N_{s2}, DS_1, DS_2, \eta, \hat{f}^1(x), X_U, X_L, D$

- 1: Construct the fitness value-based RBF surrogate model $FS \hat{f}^R(x) \leftarrow DS_1$.
- 2: Construct the error value-based RBF surrogate model $\hat{f}^\epsilon(x)$ using $\{(x, f(x) - \hat{f}^1(x)) | x \in DS_1\}$.
- 3: Build the composite surrogate model $CS \hat{f}^C(x) = \hat{f}^1(x) + \hat{f}^\epsilon(x)$.
- 4: Calculate $RMSE$ values of $\hat{f}^C(x)$ and $\hat{f}^R(x)$ on DS_2 .
- 5: **if** $RMSE_{CS} \leq RMSE_{FS}$ **then**
- 6: $\hat{f}^C(x) \leftarrow DS_1 \cup DS_2$.
- 7: $\hat{f}(x) = \hat{f}^C(x)$.
- 8: **else**
- 9: $\hat{f}^R(x) \leftarrow DS_1 \cup DS_2$.
- 10: $\hat{f}(x) = \hat{f}^R(x)$.
- 11: **end if**

Output: Final HSM $\hat{f}(x)$.

3.4. Adaptive infill strategy

The pseudo-code of the adaptive infill strategy (AIS) is shown in Algorithm 4. At first, when the individual with the best-predicted fitness value is determined, the real fitness value of the individual is evaluated by the real fitness function (Also known as the performance-based criteria). Compare the obtained real fitness value to the minimum fitness value in the database, the individual with the smaller real fitness value is set to the current best solution x_b , update the database with the best individual in the population. Then the second infill strategy is based on x_b , choose one dimension k randomly in the design space. In the chosen k th dimension, we create the upper and lower boundary around x_b using the following equations:

$$r_2 = \left(1 - \frac{cFEs - 1}{N_{mf} - 1}\right)^{\frac{1}{(1-e^{-p})(1-\frac{cFEs-1}{N_{mf}})}} \quad (18)$$

$$p = \left| \frac{f_{\max} - f_{\min}}{f_{\min}} \right| \quad (19)$$

$$\tilde{X}_U^k = x_b^k + r_2(X_U^k - X_L^k) \quad (20)$$

$$\tilde{X}_L^k = x_b^k - r_2(X_U^k - X_L^k) \quad (21)$$

Where $cFEs$ and N_{mf} denote the current number of FEs and the maximum number of extra FEs, respectively. p is the pressure factor

Algorithm 4 Adaptive infill strategy.

Input: $Pop(1), DB, D, cFEs, N_{mf}$

- 1: Select the individual $Pop(1)$ as the first infill point and evaluate the real fitness value f_1 .
- 2: **if** $f_1 < \min(DB)$ **then**
- 3: $x_b = Pop(1)$.
- 4: **else**
- 5: $x_b = x_{\min(DB)}$.
- 6: **end if**
- 7: $DB = [DB; (Pop(1), f_1)]$.
- 8: $cFEs = cFEs + 1$.
- 9: **if** $cFEs == N_{mf}$ **then**
- 10: Break.
- 11: **end if**
- 12: Randomly select a dimension $k = randi(1, D)$.
- 13: Mutate the x_b in the k th dimension by Eqs. (18-21).
- 14: Obtain $Pop(1)_m$.
- 15: Evaluate the real fitness value f_2 of $Pop(1)_m$.
- 16: **if** $f_2 < \min(DB)$ **then**
- 17: $x_b = Pop(1)_m$.
- 18: **else**
- 19: $x_b = x_{\min(DB)}$.
- 20: **end if**
- 21: $DB = [DB; (Pop(1)_m, f_2)]$.
- 22: $cFEs = cFEs + 1$.
- 23: **if** $cFEs == N_{mf}$ **then**
- 24: Break.
- 25: **end if**

Output: Infill points, $DB, cFEs$

of the mutation range. Then mutate x_b along the k th dimension with the uniform sampling in the interval $[\tilde{X}_L^k, \tilde{X}_U^k]$. When the positions of the \tilde{X}_L^k and \tilde{X}_U^k exceed the boundary, set their values as the boundary values. In the early stage of the adaptive infill strategy, the value of r_2 is large, so that the mutation range around x_b is at a large level, so the new solution obtained by mutating x_b is far away from x_b on the k th dimension, thereby increasing the exploration ability of the entire search process. As the number of iterations increases, the value of r_2 gradually decreases, so the new solution obtained by mutating x_b is as close as possible to x_b on the k th dimension, thereby enhancing exploitation ability of the evolutionary search. Therefore, through the second infill criteria, the proposed adaptive infill strategy can achieve a good balance between exploration and exploitation in the evolutionary search process. In addition, the larger the pressure factor, the more significant the difference between the database's maximum and minimum function values (f_{\max}, f_{\min}). When the pressure factor increases, the adaptive infill strategy will improve the mutation range, thereby adaptively improving the exploration ability of SAEA-HAS. After the mutated solution is obtained, the real fitness value of the mutated individual is evaluated. Then compare the obtained real fitness value to the minimum fitness value in the database, and the individual with the smaller real fitness value is set to the current best solution x_b . The database is updated with the mutated individual in the population. Finally, output the infill points, the current number of real fitness evaluations and the updated database.

3.5. Complexity analysis

The computational complexity of an algorithm indicates the number of resources required to run it. The computational complexity of the main steps in SAEA-HAS is shown in Table 1, in which N_D refers to

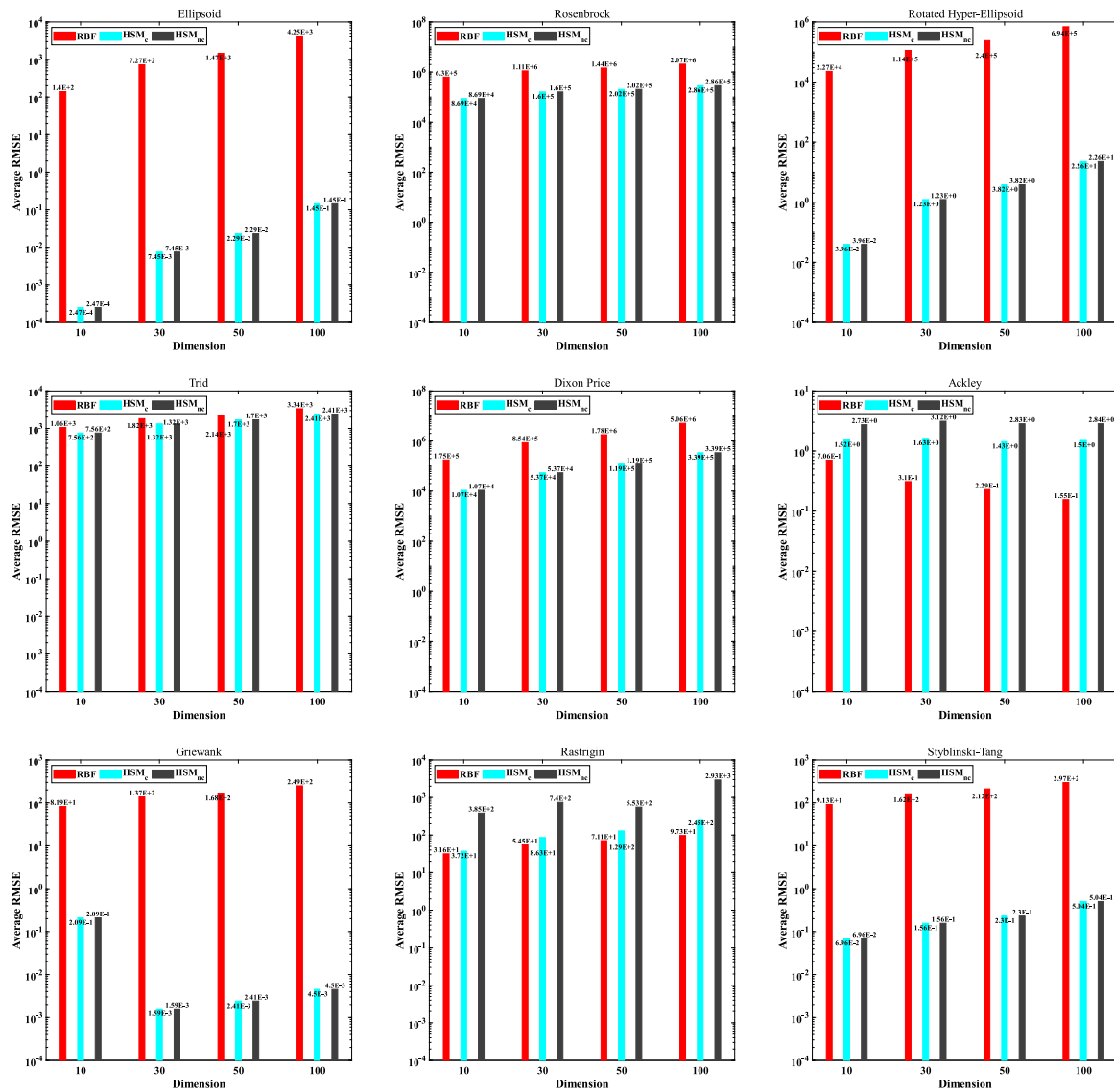


Fig. 2. The average root mean square errors of the three surrogate models on the nine test functions.

Table 1

Computational complexity of SAEA-HAS.

HDMR	HSM	Evaluation	Infill Strategy
$O(DN_D)$	$O(MN_{s2})$	$O(\frac{N_{Pop}N_{mL}}{2})$	$O(N_{mf})$

the number of training samples evaluated by real fitness function in the D th component of the HDMR model. M indicates the number of surrogate models employed in HSM, its value is 2 (the fitness value-based surrogate and the composite surrogate). N_{s2} is the size of training subset 2. The notation N_{Pop} represents the number of parent population and offspring evaluated by HSM in each iteration. It is worth noting that for expensive black-box optimization problems, the computational costs of the real fitness evaluation are much larger than that of the surrogate modeling, fitness prediction and optimization iteration in the SAEA algorithm. Therefore, compared to the other three parts in Table 1, the computational cost of evaluation is relatively small in solving expensive optimization problems.

Table 2

Average RMSE and average number of training samples (in brackets) for HSM_c and second-order HDMR model on the Ackley function.

Function	D	HSM_c	Second order HDMR
Ackley	10	1.52E+00(1.21E+02)	2.40E+00(3.82E+02)
	30	1.63E+00(3.31E+02)	7.02E+00(2.49E+03)
	50	1.43E+00(4.51E+02)	9.35E+00(6.54E+03)
	100	1.50E+00(9.01E+02)	1.24E+01(2.52E+04)

4. Experimental studies

4.1. Experimental setup

To test the performance of SAEA-HAS, twelve benchmark functions widely used in evolutionary optimization (Liu, Liu, & Tan, 2023; Suganthan et al., 2005; Surjanovic & Bingham, 2013) are employed to compare SAEA-HAS with other well-known SAEAs. The twelve benchmark test problems have different characteristics, including multi-modal, bowl-shaped uni-modal, valley-shaped uni-modal and shifted global optimum. The details of those functions can be found in the Appendix

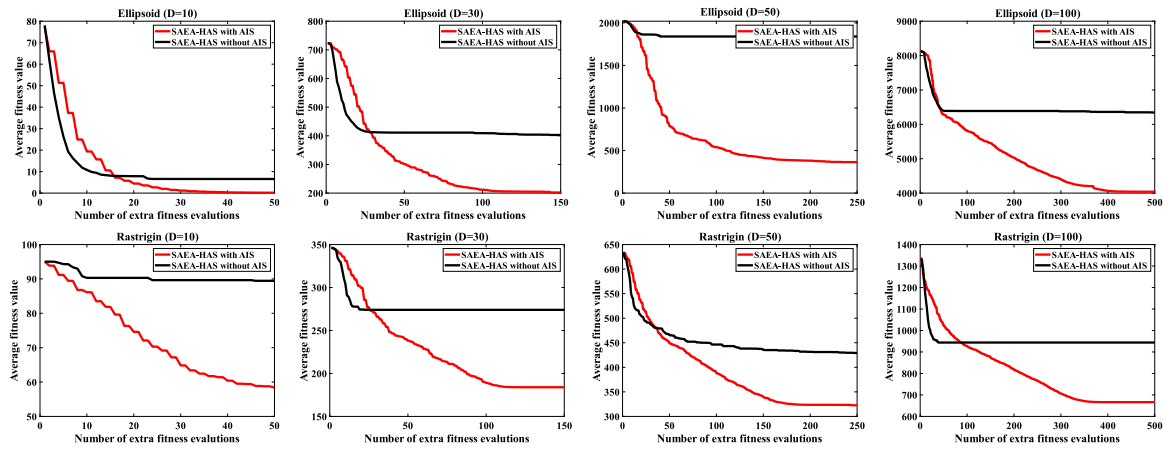


Fig. 3. Convergence curves of the two SAEAs on the two test functions under different dimensions.

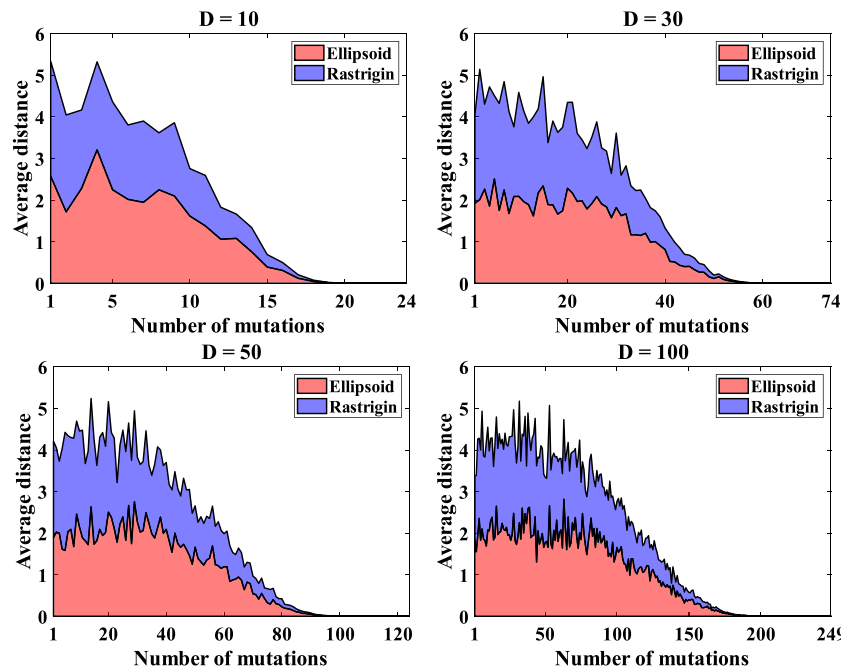


Fig. 4. The exploration and exploitation transformation of the AIS on the two test functions under different dimensions.

Table 3

The average optimal fitness values of the two SAEAs on two test functions under different dimensions.

Function	D	SAEA-HAS	SAEA-HASw
Ellipsoid	10	1.69E-01 ± 2.45E-01	6.57E+00 ± 1.09E+01(+)
	30	2.02E+02 ± 1.74E+02	4.03E+02 ± 2.99E+02(+)
	50	3.64E+02 ± 3.18E+02	1.84E+03 ± 3.83E+02(+)
	100	4.04E+03 ± 9.08E+02	6.34E+03 ± 2.57E+03(+)
Rastrigin	10	5.84E+01 ± 1.44E+01	8.94E+01 ± 1.37E+01(+)
	30	1.84E+02 ± 2.62E+01	2.74E+02 ± 2.23E+01(+)
	50	3.23E+02 ± 2.74E+01	4.29E+02 ± 4.29E+01(+)
	100	6.66E+02 ± 1.09E+02	9.44E+02 ± 9.52E+01(+)
w/t/l		NA	8\0\0

(Table A.1). Five existing well-known algorithms, including SAEA-RFS (Fu et al., 2020), SAEA-UGC (Liu et al., 2021), HESNFO (Yu, Liang, Wu et al., 2022), LSADE (Kudela & Matousek, 2023) and aRBF-NFO (Yu, Liang, Zhao et al., 2022) are employed to compare with the proposed SAEA-HAS. For a fair experimental analysis, the following experimental settings are given.

- For the evolutionary optimization algorithm, a generic GA (Mirjalili, 2019) using the simulated binary crossover (SBX), polynomial mutation, and tournament selection is used in SAEA-HAS, HESNFO, SAEA-UGC and aRBF-NFO, the population size is set to 100. The crossover and mutation probabilities are set to 1 and 1/D, respectively. The number of folds for HESNFO and SAEA-UGC algorithms is set to the minimum of all fold numbers (D = 30, 50, 100). D refers to the dimension of the fitness function. Differential algorithm (DE) (Qin, Huang, & Suganthan, 2009) is used in SAEA-RFS and LSADE (Static rule); the training sample set is used to initialize the population in LSADE, the settings of algorithm parameters of the two SAEAs are consistent with the original paper.
- The training samples of SAEA-HAS consists of two parts. The first training set was for building the first-order RBF-HDMR and the second training set was for the contrastive analysis. The values of convergence criteria ϵ_1 and the sampling factor β are set to 0.01 and 0.5, respectively. The RBF-HDMR model-building process determines the number of sample points in the first training set.

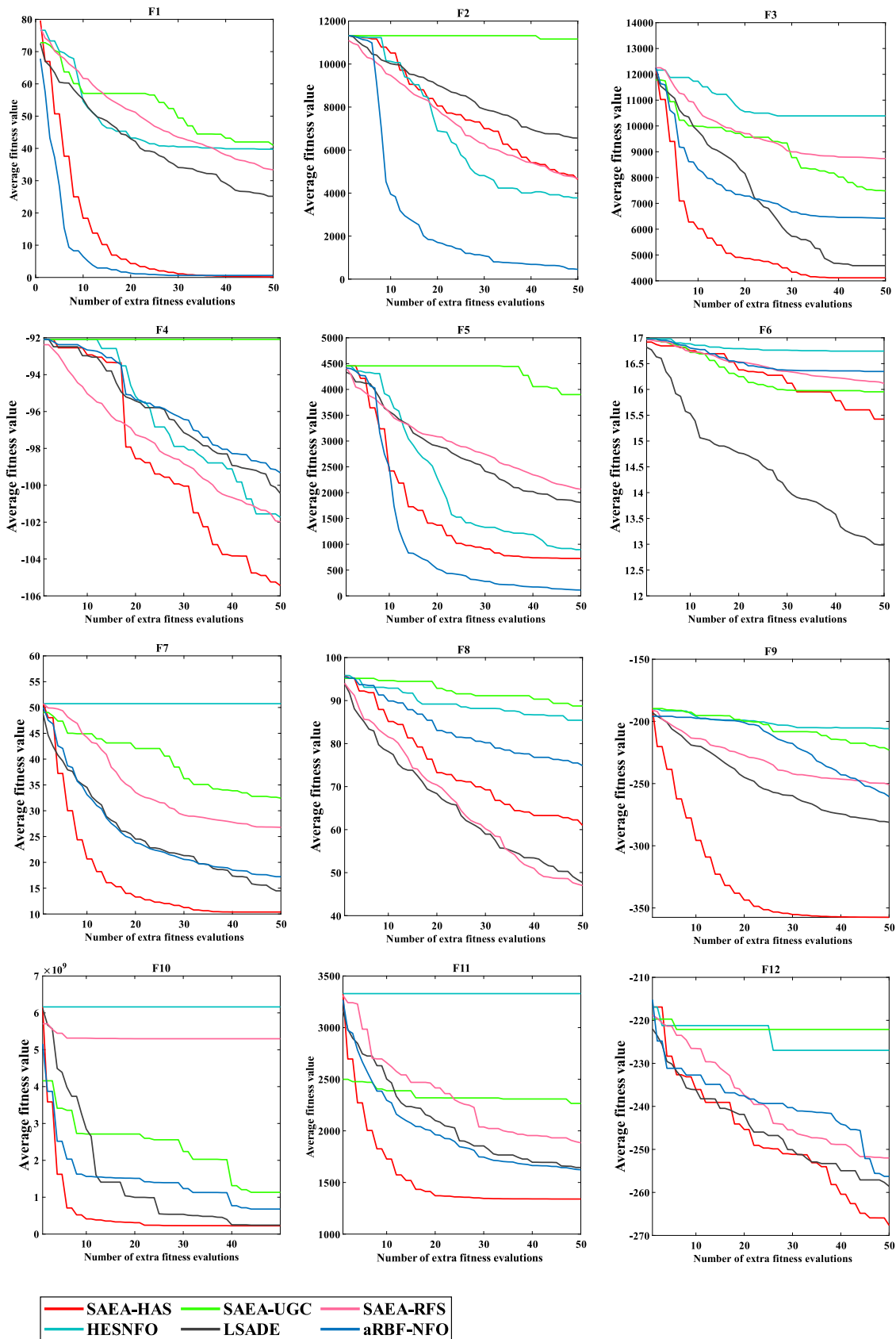


Fig. 5. Convergence curves of different SAEAs for test problems with 10 dimensions.

Table 4
Comparisons between the proposed algorithm and other SAEAs on test problems with 10 dimensions.

Function	ID	Metric	SAEA-HAS	HESNFO	SAEA-UGC	LSADE	SAEA-RFS	aRBF-NFO
Ellipsoid	F1	Mean	1.767E-01	3.975E+01	4.097E+01	2.516E+01	3.336E+01	6.292E-01
		Std.	1.852E-01	1.486E+01	1.219E+01	1.311E+01	6.670E+00	3.633E-01
Rosenbrock	F2	Mean	4.629E+03	3.778E+03	1.116E+04	6.559E+03	4.671E+03	4.543E+02
		Std.	2.802E+03	1.891E+03	6.931E+02	2.135E+03	1.413E+03	2.592E+02
Rotated Hyper-Ellipsoid	F3	Mean	4.116E+03	1.039E+04	7.486E+03	4.588E+03	8.734E+03	6.434E+03
		Std.	3.330E+03	2.254E+03	1.942E+03	1.782E+03	2.726E+03	2.225E+03
Trid	F4	Mean	-1.054E+02	-1.017E+02	-9.209E+01	-1.004E+02	-1.020E+02	-9.933E+01
		Std.	1.176E+01	8.945E+00	4.714E+00	7.314E+00	4.037E+00	6.092E+00
Dixon-Price	F5	Mean	7.244E+02	8.958E+02	3.900E+03	1.814E+03	2.067E+03	1.131E+02
		Std.	7.379E+02	6.297E+02	1.142E+03	7.222E+02	5.698E+02	8.215E+01
Ackley	F6	Mean	1.542E+01	1.674E+01	1.595E+01	1.299E+01	1.612E+01	1.635E+01
		Std.	1.118E+00	4.394E-01	4.600E-01	2.069E+00	4.257E-01	4.019E-01
Griewank	F7	Mean	1.038E+01	5.074E+01	3.243E+01	1.448E+01	2.679E+01	1.722E+01
		Std.	9.289E+00	3.010E+00	8.603E+00	4.781E+00	9.712E+00	5.461E+00
Rastrigin	F8	Mean	6.100E+01	8.543E+01	8.874E+01	4.772E+01	4.701E+01	7.497E+01
		Std.	1.075E+01	1.402E+01	1.511E+01	1.293E+01	1.088E+01	1.092E+01
Styblinski-Tang	F9	Mean	-3.576E+02	-2.058E+02	-2.231E+02	-2.811E+02	-2.509E+02	-2.612E+02
		Std.	2.754E+01	1.269E+01	2.204E+01	2.279E+01	2.578E+01	2.783E+01
Shifted Rosenbrock	F10	Mean	2.243E+08	6.161E+09	1.133E+09	2.425E+08	5.298E+09	6.786E+08
		Std.	4.554E+08	2.653E+09	7.140E+08	1.856E+08	2.253E+09	3.439E+08
Shifted Rotated Griewank	F11	Mean	1.340E+03	3.329E+03	2.266E+03	1.645E+03	1.884E+03	1.623E+03
		Std.	5.365E+02	2.068E+02	1.877E+02	3.573E+02	6.069E+02	3.932E+02
Shifted Rastrigin	F12	Mean	-2.677E+02	-2.270E+02	-2.221E+02	-2.586E+02	-2.520E+02	-2.563E+02
		Std.	2.175E+01	1.069E+01	1.044E+01	1.890E+01	1.415E+01	1.891E+01
<i>w/t/l</i>			NA	9\3\0	11\1\0	7\3\2	9\2\1	9\1\2
Average Ranking			1.5	4.875	5.1667	2.6667	3.875	2.9167
Adjusted <i>p</i> -value			NA	0.00001	0.000002	0.12663	0.001873	0.063617

The samples in the second training set are generated by the *LHS* in the input domain. According to Wang et al. (2017), the amount of data in the second training set is five times the dimension of the fitness function, which is represented by *5D*. The training sample set for the other five comparison algorithms is the same as that of SAEA-HAS.

- The RBF model with Gaussian kernel function is adopted as the base surrogate in this work. Because of the ensemble of surrogates included in SAEA-UGC, the kernel functions of the other two RBF models use Multi-quadric and Thin plate spline, respectively. The kernel parameter of the RBF model in SAEA-HAS, SAEA-UGC, SAEA-RFS, aRBF-NFO and LSADe is set to 1.
- To avoid randomness, the six SAEAs perform 20 times on each benchmark test problem and the average optimization results with standard deviation are obtained. Wilcoxon's rank-sum test (Significance level $\alpha = 0.05$) is used to compare SAEA-HAS and other comparison algorithms. Moreover, the Friedman test with the Bergmann-Hommel *post-hoc* test (Significance level $\alpha = 0.05$) is further used to conduct multiple comparisons of different SAEAs.

All numerical experiments were carried out on a computer with the AMD processor (16-Core, 2.40 GHz). The computer's RAM is 1 TB.

4.2. Accuracy analysis of the hierarchical surrogate model

In this section, we employ nine commonly used test functions in surrogate modeling, including Ellipsoid, Rosenbrock, Rotated Hyper-Ellipsoid, Trid, Dixon Price, Ackley, Griewank, Rastrigin and Styblinski-Tang, to compare the global prediction accuracy of the stand-alone RBF surrogate and the HSM. Ellipsoid, Rosenbrock, Rotated Hyper-Ellipsoid, Trid and Dixon Price are uni-modal functions while Ackley, Griewank, Rastrigin and Styblinski-Tang are multi-modal test functions. In order to verify the effectiveness of the contrastive analysis, the HSM model with contrastive analysis HSM_c and the HSM model without contrastive analysis HSM_{nc} are both compared on these functions.

The training data generated by *LHS* is employed to construct the RBF model, and the number of training samples of these surrogates is the same. To remove the effect of random sampling, 20 different training sets are generated for comparison. Randomly sample 1000 prediction points to test the surrogate models constructed with the training set. The global prediction accuracy of these surrogates is then evaluated by computing the mean root mean square error (RMSE).

As shown in Fig. 2, compared to the stand-alone RBF model, the average RMSE values of HSM on the nine test functions suggest that HSM has superiority in global prediction accuracy. In most test problems (7 out of 9), the global prediction accuracy of HSM is much higher than that of the stand-alone RBF model under different dimensions (10, 30, 50, 100), which suggests that the proposed HSM has good global

Table 5
Comparisons between the proposed algorithm and other SAEAs on test problems with 30 dimensions.

Function	ID	Metric	SAEA-HAS	HESNFO	SAEA-UGC	LSADE	SAEA-RFS	aRBF-NFO
Ellipsoid	F1	Mean	2.573E+02	2.525E+02	2.913E+02	4.837E+02	3.339E+02	1.72E+02
		Std.	1.258E+02	6.092E+01	1.245E+02	8.471E+01	5.072E+01	8.23E+01
Rosenbrock	F2	Mean	1.677E+04	2.716E+04	2.002E+04	3.430E+04	1.888E+04	6.331E+04
		Std.	6.816E+03	5.668E+03	5.665E+03	2.213E+03	2.285E+03	3.413E+04
Rotated Hyper-Ellipsoid	F3	Mean	7.439E+04	1.191E+05	8.110E+04	5.093E+04	1.051E+05	9.934E+04
		Std.	9.563E+03	1.066E+03	8.108E+03	1.266E+04	7.337E+03	2.135E+04
Trid	F4	Mean	-4.585E+02	-4.321E+02	-4.544E+02	-4.335E+02	-4.545E+02	-4.333E+02
		Std.	1.974E+01	4.436E+00	1.686E+01	4.531E+00	4.365E+00	3.419E+00
Dixon-Price	F5	Mean	1.052E+04	2.088E+04	1.361E+04	3.121E+04	1.998E+04	4.718E+04
		Std.	5.983E+03	4.213E+03	4.984E+03	6.570E+03	1.746E+03	2.067E+04
Ackley	F6	Mean	1.642E+01	1.728E+01	1.665E+01	1.540E+01	1.637E+01	1.832E+01
		Std.	1.460E-01	1.158E-02	1.073E-01	1.027E+00	9.889E-02	8.937E-01
Griewank	F7	Mean	1.093E+02	1.642E+02	1.176E+02	8.779E+01	1.295E+02	1.532E+02
		Std.	9.908E+00	1.341E-01	8.425E+00	1.730E+01	1.729E+01	5.181E+01
Rastrigin	F8	Mean	1.833E+02	3.313E+02	2.188E+02	2.090E+02	1.402E+02	2.302E+02
		Std.	2.397E+01	2.520E+01	2.052E+01	2.495E+01	2.534E+01	2.875E+01
Styblinski-Tang	F9	Mean	-8.842E+02	-4.713E+02	-7.851E+02	-7.263E+02	-6.529E+02	-7.808E+02
		Std.	1.783E+02	3.639E+01	1.343E+02	5.066E+01	4.676E+01	6.892E+01
Shifted Rosenbrock	F10	Mean	2.029E+10	3.811E+10	2.457E+10	5.514E+09	3.082E+10	6.643E+09
		Std.	4.772E+09	2.124E+06	3.328E+09	3.005E+09	4.256E+09	3.338E+09
Shifted Rotated Griewank	F11	Mean	5.817E+03	1.136E+04	7.478E+03	6.454E+03	7.088E+03	8.207E+03
		Std.	2.727E+03	7.097E+02	1.755E+03	3.146E+02	7.134E+02	7.632E+02
Shifted Rastrigin	F12	Mean	-1.441E+01	1.406E+02	2.279E+01	4.807E+01	4.404E+01	6.749E+00
		Std.	2.904E+01	3.406E+01	2.036E+01	2.252E+01	3.076E+01	4.243E+01
$w/t/l$			NA	11\1\0	7\5\0	8\0\4	8\3\1	8\2\2
Average Ranking			1.7083	5.25	3.25	3.1667	3.4583	4.1667
Adjusted p -value			NA	0.000004	0.043538	0.05621	0.021947	0.001288

prediction accuracy on both uni-modal and multi-modal problems. Since there are high-order interactions between design variables in the Rastrigin and Ackley functions, the stand-alone RBF model provides better prediction results than HSM on the two functions. From the average RMSE results on the Rastrigin and Ackley functions, we can observe that the global prediction accuracy of HSM_c is higher than that of HSM_{nc} . It means that the contrastive analysis can effectively identify the test problem with high-order interactions between input variables, thereby improving the robustness of HSM.

4.3. Order selection of HDMR model

In general, the expansion of HDMR to the second order is considered sufficient to represent the output. However, when the fitness function is highly nonlinear, the number of sample points required to train the second-order HDMR model increases sharply with the increase of the model order.

Take the Ackley function (highly nonlinear) as an example, we calculate the average RMSE and the average number of training samples for HSM_c and second-order HDMR model on the Ackley function (based on 20 independent runs). As listed in Table 2, the second-order HDMR model requires far more sample points than HSM_c , and its prediction accuracy is also lower than that of HSM_c . This gap expands as the function dimension increases. For expensive optimization problems, the calculation cost of the fitness value is high. Therefore, in the proposed SAEA-HAS, we choose to use the first-order HDMR model to maintain the computational efficiency of HSM_c .

4.4. Analysis of the adaptive infill strategy

In this work, the adaptive infill strategy (AIS) is integrated into SAEA-HAS with the aim of enhancing its exploration and exploitation abilities. It is necessary to investigate the influence of the AIS on SAEA-HAS. This section employs the uni-modal test problem Ellipsoid and the multi-modal test problem Rastrigin as test examples. To analyze the performance of the proposed AIS, we compare the performance of SAEA-HAS with AIS and SAEA-HAS with only the performance-based criteria on the test examples under different dimensions (10, 30, 50, 100). Each algorithm performs 20 times independently to avoid randomness. The number of extra FEs is five times the dimension of the fitness function. Other parameters of the SAEA-HAS algorithm are the same as in Section 4.1. Convergence curves of the average fitness values of the two algorithms on different test problems are obtained to see the impact of AIS on the convergence performance. In addition, to observe the shift in exploration and exploitation of the AIS strategy as the number of FEs increases, we also record average changes in the distance between the current best solution and the mutated solution. The test results are shown in Figs. 3, 4 and Table 3.

As shown in Fig. 3, compared with SAEA-HAS without AIS, SAEA-HAS with AIS shows better performance in terms of convergence on Ellipsoid and Rastrigin functions with different dimensions (10, 30, 50, 100). SAEA-HAS with only performance-based infill criteria suffers from premature convergence of optimization results. The Wilcoxon rank sum test results listed in Table 3 indicate that AIS can enhance

Table 6
Comparisons between the proposed algorithm and other SAEAs on test problems with 50 dimensions.

Function	ID	Metric	SAEA-HAS	HESNFO	SAEA-UGC	LSADE	SAEA-RFS	aRBF-NFO
Ellipsoid	F1	Mean	4.239E+02	8.045E+02	5.476E+02	1.740E+03	9.658E+02	9.144E+02
		Std.	4.509E+02	8.673E+01	3.980E+02	1.144E+02	7.174E+01	2.188E+02
Rosenbrock	F2	Mean	3.569E+04	5.317E+04	4.078E+04	6.283E+04	3.302E+04	3.786E+05
		Std.	1.082E+04	7.375E+03	8.283E+03	1.200E+03	2.478E+03	2.432E+05
Rotated Hyper-Ellipsoid	F3	Mean	2.077E+05	3.306E+05	2.335E+05	2.185E+05	2.985E+05	3.945E+05
		Std.	2.108E+04	1.332E+03	1.675E+04	3.935E+04	1.635E+04	7.088E+04
Trid	F4	Mean	-8.126E+02	-7.712E+02	-8.039E+02	-7.777E+02	-8.086E+02	-7.756E+02
		Std.	1.784E+01	3.081E+00	1.429E+01	5.997E+00	5.498E+00	3.922E+00
Dixon-Price	F5	Mean	4.405E+04	7.546E+04	4.877E+04	1.105E+05	5.660E+04	3.394E+05
		Std.	2.043E+04	1.093E+04	1.772E+04	7.189E+03	4.497E+03	1.509E+05
Ackley	F6	Mean	1.651E+01	1.733E+01	1.668E+01	1.600E+01	1.635E+01	1.927E+01
		Std.	2.140E-01	5.540E-03	1.690E-01	4.040E-01	1.078E-01	3.433E-01
Griewank	F7	Mean	1.810E+02	2.767E+02	2.040E+02	1.699E+02	2.171E+02	4.491E+02
		Std.	1.473E+01	7.276E-02	1.120E+01	1.607E+01	1.989E+01	5.543E+01
Rastrigin	F8	Mean	3.298E+02	4.082E+02	3.511E+02	4.277E+02	2.524E+02	4.325E+02
		Std.	3.318E+01	3.652E+01	2.998E+01	6.345E+01	5.348E+01	3.373E+01
Styblinski-Tang	F9	Mean	-1.281E+03	-7.056E+02	-1.195E+03	-1.013E+03	-1.062E+03	-1.241E+03
		Std.	2.374E+02	2.348E+01	2.009E+02	9.559E+01	9.675E+01	6.493E+01
Shifted Rosenbrock	F10	Mean	3.285E+10	6.013E+10	4.103E+10	2.482E+10	5.265E+10	6.028E+10
		Std.	1.022E+10	4.765E+06	6.562E+09	1.555E+10	2.479E+09	3.165E+09
Shifted Rotated Griewank	F11	Mean	8.670E+03	1.610E+04	9.785E+03	8.691E+03	1.066E+04	1.186E+04
		Std.	2.714E+03	3.846E+02	2.117E+03	7.191E+02	9.815E+02	5.939E+02
Shifted Rastrigin	F12	Mean	1.776E+02	4.365E+02	2.164E+02	3.685E+02	3.299E+02	2.964E+02
		Std.	4.692E+01	3.384E+01	3.841E+01	3.384E+01	1.725E+01	7.014E+01
<i>w/t/l</i>			NA	12\0\0	6\6\0	7\2\3	8\2\2	11\1\0
Average Ranking			1.5	4.9167	2.8333	3.5	3.1667	5.0833
Adjusted <i>p</i> -value			NA	0.000008	0.080856	0.008829	0.029096	0.000003

the convergence performance of the proposed SAEA-HAS. As shown in Fig. 4, we record average changes in the distance (in the mutation dimension) between the current best solution and the mutated solution on Ellipsoid and Rastrigin functions. From Fig. 4, we can observe that in the early stage of the adaptive infill strategy, the mutation distance is at a large level, which is beneficial for the exploration of the surrogate-assisted evolutionary search. With the number of FEs increases, the distance between the current best solution and the mutated solution gradually decreases, indicating that AIS can effectively achieve the balance between exploration and exploitation of the surrogate-assisted evolutionary search. In addition, the distance change of the Ellipsoid function is greater than that of the Rastrigin function because the pressure factor of the Ellipsoid function is larger. In this case, the AIS strategy will increase the mutation range, thereby adaptively improving the exploration ability of SAEA-HAS on the test function.

4.5. Comparison on low dimensional problems

To investigate the optimization performance of SAEA-HAS on low-dimensional problems ($D = 10$), we compare the proposed SAEA-HAS with HESNFO, SAEA-UGC, LSAD, SAEA-RFS and aRBF-NFO. The number of extra FEs is five times the dimension of the fitness function. All the experimental settings are introduced in Section 4.1. The statistical results are shown in Table 4, Fig. 5. The symbols “+, ≈, -” in Table 4 suggest that from the result of the Wilcoxon rank-sum test of the test problems, SAEA-HAS is better than, close to, or worse than the

compared algorithm, respectively. The twelve test problems’ Wilcoxon rank-sum test results are presented by the symbols “ w, t, l ”. This indicates that SAEA-HAS performs better on w test problems, similar on t test problems, and worse on l test problems than its competitor. To analyze the influence of the characteristics of different test problems on the performance of the six SAEAs, the twelve benchmark test problems are divided into three categories, uni-modal (F1-F5), multi-modal (F6-F9) and shifted global optimum (F10-F12).

As for the case with 10 dimension test problems, the test results listed in Table 4 suggest that SAEA-HAS shows better overall performance than the other five SAEAs on low-dimensional test problems. According to the Friedman test results (SAEA-HAS is selected as the control method), SAEA-HAS has the minimum average ranking value (1.5). Moreover, SAEA-HAS produces the best average optimization results (Shown in bold) on 8 of the 12 test problems.

Compared to SAEA-UGC and SAEA-RFS, SAEA-HAS and aRBF-NFO have superiority in obtaining better optimal solutions on uni-modal test functions with 10 dimensions (F1-F5) based on Wilcoxon’s rank-sum test results. The convergence curves of all the algorithms on all the test problems with 10 dimensions are plotted in Fig. 5. The convergence performance of SAEA-HAS and aRBF-NFO is better than other comparison algorithms in uni-modal test functions. SAEA-HAS and LSAD show better performance than HESNFO, SAEA-UGC and aRBF-NFO on multi-modal test functions (F6-F9) (See Table 4). SAEA-HAS and LSAD have similar performance on the multi-modal functions with low dimensions. The convergence performance of SAEA-HAS is better

Table 7
Comparisons between the proposed algorithm and other SAEAs on test problems with 100 dimensions.

Function	ID	Metric	SAEA-HAS	HESNFO	SAEA-UGC	LSADE	SAEA-RFS	aRBF-NFO
Ellipsoid	F1	Mean	3.377E+03	2.481E+03	4.021E+03	7.573E+03	4.244E+03	5.192E+03
		Std.	1.438E+03	6.420E+01	1.833E+03	2.286E+02	2.107E+02	1.066E+03
Rosenbrock	F2	Mean	7.422E+04	1.232E+05	1.257E+05	1.345E+05	6.926E+04	1.224E+06
		Std.	1.676E+04	1.059E+04	1.141E+04	1.632E+03	5.526E+03	3.865E+05
Rotated Hyper-Ellipsoid	F3	Mean	8.629E+05	1.326E+06	1.419E+06	1.109E+06	1.176E+06	2.058E+06
		Std.	6.037E+04	5.225E+03	1.402E+04	1.491E+05	6.576E+04	2.592E+05
Trid	F4	Mean	-1.712E+03	-1.622E+03	-1.577E+03	-1.626E+03	-1.690E+03	-1.615E+03
		Std.	3.439E+01	4.178E+00	2.091E+01	4.552E+00	8.442E+00	5.549E+00
Dixon-Price	F5	Mean	2.775E+05	3.988E+05	4.595E+05	4.839E+05	2.354E+05	2.311E+06
		Std.	5.556E+04	3.294E+04	6.522E+04	5.465E+03	1.533E+04	5.357E+05
Ackley	F6	Mean	1.640E+01	1.817E+01	1.800E+01	1.652E+01	1.700E+01	1.989E+01
		Std.	6.619E-02	2.048E-01	1.871E-01	1.268E-01	1.848E-01	2.566E-01
Griewank	F7	Mean	3.660E+02	5.579E+02	6.539E+02	4.360E+02	4.360E+02	1.175E+03
		Std.	2.436E+01	2.031E-02	1.217E+01	3.978E+01	3.010E+01	1.427E+02
Rastrigin	F8	Mean	6.568E+02	1.131E+03	1.368E+03	1.156E+03	4.650E+02	1.007E+03
		Std.	1.041E+02	1.115E+02	1.641E+02	5.017E+01	8.800E+01	5.501E+01
Styblinski-Tang	F9	Mean	-2.156E+03	-1.232E+03	-7.699E+02	-1.443E+03	-1.959E+03	-2.135E+03
		Std.	3.527E+02	3.955E+01	1.741E+02	1.466E+02	1.083E+02	3.251E+02
Shifted Rosenbrock	F10	Mean	5.379E+10	1.063E+11	1.325E+11	8.788E+10	1.089E+11	1.075E+11
		Std.	7.255E+09	1.446E+09	4.663E+09	5.352E+09	4.900E+09	5.637E+06
Shifted Rotated Griewank	F11	Mean	4.147E+04	4.216E+04	4.626E+04	4.694E+04	2.604E+04	4.386E+04
		Std.	4.158E+03	4.601E+02	4.771E+03	4.046E+03	5.272E+02	3.794E+03
Shifted Rastrigin	F12	Mean	7.495E+02	1.232E+03	1.474E+03	1.308E+03	1.112E+03	1.339E+03
		Std.	6.172E+01	2.273E+01	5.680E+01	1.213E+02	8.570E+01	1.326E+02
<i>w/t/l</i>			NA	10\1\1	11\1\0	12\0\0	8\1\3	10\2\0
Average Ranking			1.4167	3.5417	5	3.875	2.375	4.7917
Adjusted <i>p</i> -value			NA	0.005398	0.000003	0.001288	0.209568	0.00001

Table 8
Design variables of the Yagi-Uda antenna design problem.

Design variable	Initial design	Range
x_1 (m)	0.5 λ	[0.4 λ , 0.6 λ]
x_2 (m)	0.495 λ	[0.35 λ , 0.495 λ]
x_3 (m)	0.495 λ	[0.35 λ , 0.495 λ]
x_4 (m)	0.495 λ	[0.35 λ , 0.495 λ]
x_5 (m)	0.495 λ	[0.35 λ , 0.495 λ]
x_6 (m)	0.3 λ	[0.05 λ , 0.3 λ]
x_7 (m)	0.25 λ	[0.05 λ , 0.23 λ]
x_8 (m)	0.25 λ	[0.05 λ , 0.23 λ]
x_9 (m)	0.25 λ	[0.05 λ , 0.23 λ]
x_{10} (m)	0.25 λ	[0.05 λ , 0.23 λ]

than that of the compared algorithms on Griewank and Styblinski-Tang test functions. In addition, on these three test functions with shifted global optimum (F10-F12), the optimization results obtained by SAEA-HAS are better than the other five comparison algorithms. The test results shown in Table 4 and Fig. 5 indicate that SAEA-HAS has better robustness and convergence ability on low-dimensional test problems than the compared algorithms.

4.6. Comparison on medium and high dimensional problems

To investigate the optimization performance of SAEA-HAS on medium and high dimensional problems ($D = 30, 50, 100$), we employ

HESNFO, SAEA-UGC, LSADe, SAEA-RFS and aRBF-NFO to compare with the proposed SAEA-HAS. The number of extra FEs is five times the dimension of the fitness function. All the experimental settings are introduced in Section 4.1.

As shown in Table 5, SAEA-HAS obtains the best average optimization results on 3 out of the 5 uni-modal test problems with 30 dimensions (F1-F5). SAEA-HAS and SAEA-UGC have similar convergence performance on the 5 uni-modal test functions. As for multi-modal test problems (F6-F9) with 30 dimensions, Wilcoxon’s rank-sum test results (See Table 5) suggest that SAEA-HAS is better than HESNFO, SAEA-UGC, SAEA-RFS and aRBF-NFO in terms of the obtained average optimal results. SAEA-HAS and LSADe show similar performance on multi-modal functions with 30 dimensions. SAEA-HAS and aRBF-NFO have similar convergence performance on the test functions with shifted global optimum (F10-F12). The Friedman test results listed in Table 5 indicate that the overall performance of SAEA-HAS is better than the other five algorithms.

In the case with 50 dimensions, Wilcoxon’s rank-sum test results (See Table 6) suggest that SAEA-HAS and SAEA-RFS show similar performance on the test problems F2 and F4. SAEA-HAS and SAEA-UGC show better convergence performance than the other four SAEAs on the 5 uni-modal test functions with 50 dimensions. SAEA-HAS, LSADe and SAEA-RFS show similar performance on multi-modal functions with 50 dimensions. As for the complicated multi-modal test function with 50 dimensions (F9), SAEA-HAS offers better performance than HESNFO, LSADe and SAEA-RFS. SAEA-HAS and LSADe have similar

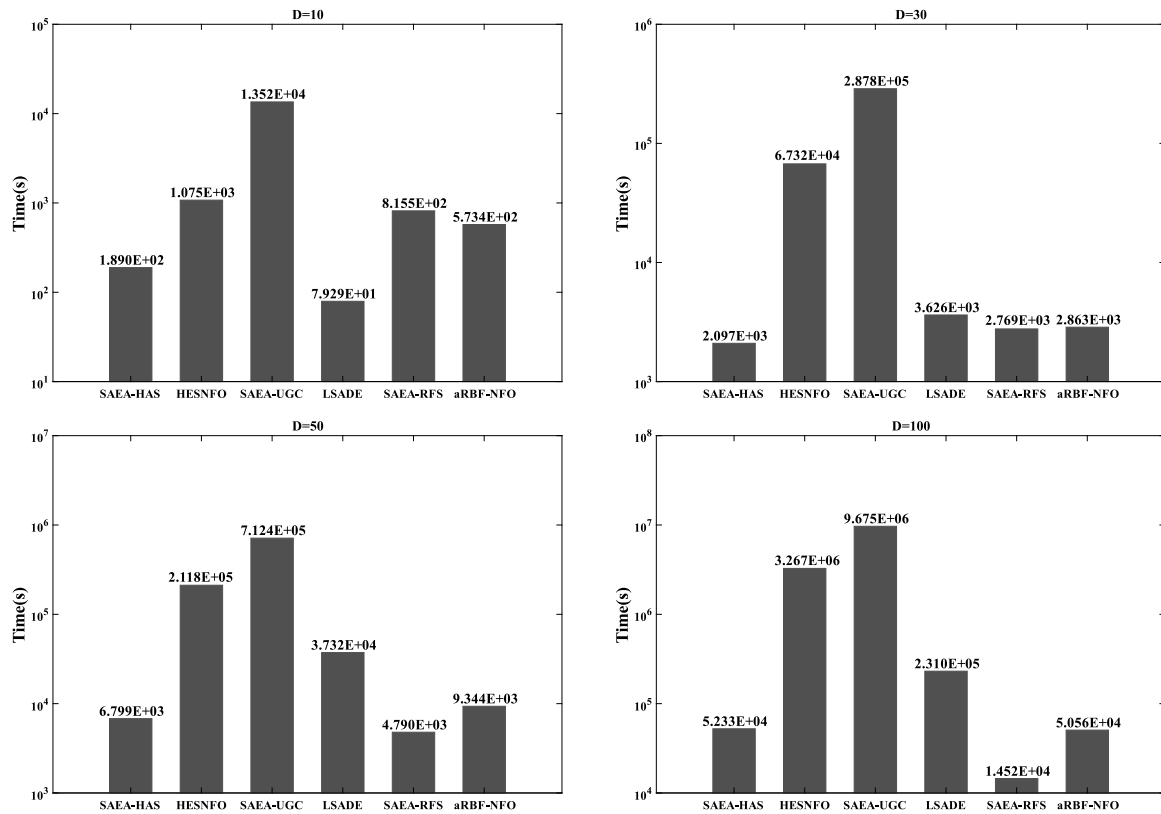


Fig. 6. Total computation time (s) of different SAEAs on the twelve benchmark test problems under different dimensions.

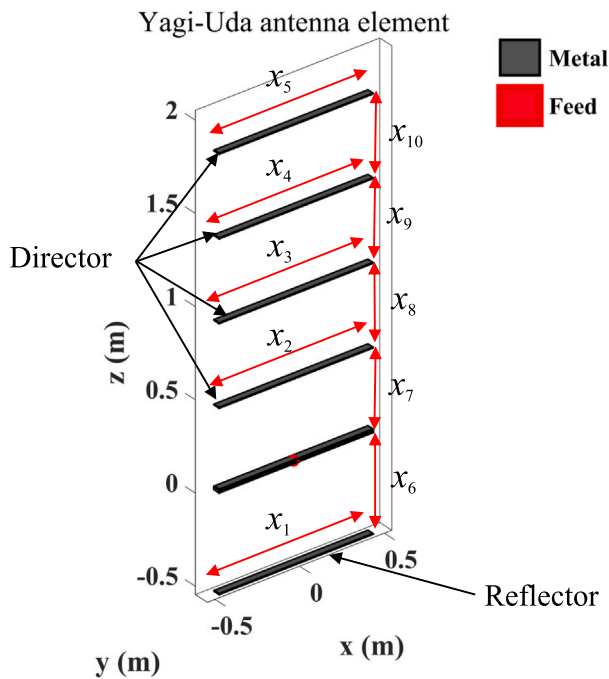


Fig. 7. The geometry of the Yagi-Uda antenna.

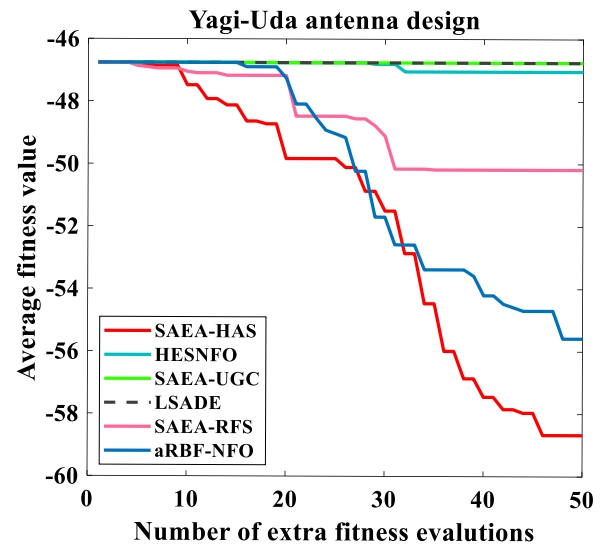


Fig. 8. Convergence curves of different SAEAs for the Yagi-Uda antenna design problem.

convergence performance on the three shifted test problems (F10-F12). The Friedman test results listed in Table 6 show that SAEA-HAS has the minimum average ranking on the test functions with 50 dimensions, which suggests that SAEA-HAS shows better adaptability to test problems with different characteristics than the other five SAEAs.

As for the case with high-dimension test problems ($D = 100$), SAEA-HAS obtains the best average optimal fitness on 7 of the 12 test problems. SAEA-HAS performs better than or similar to SAEA-RFS on 9 of the 12 test functions (See Table 7). The performance of SAEA-HAS on valley-shaped test functions with high-dimension (F2, F5) is unsatisfactory. The Friedman test results listed in Table 7 show that SAEA-HAS has better overall performance in obtaining optimization results than compared algorithms, indicating that SAEA-HAS shows better robustness and convergence ability than compared algorithms on high dimensional test problems.

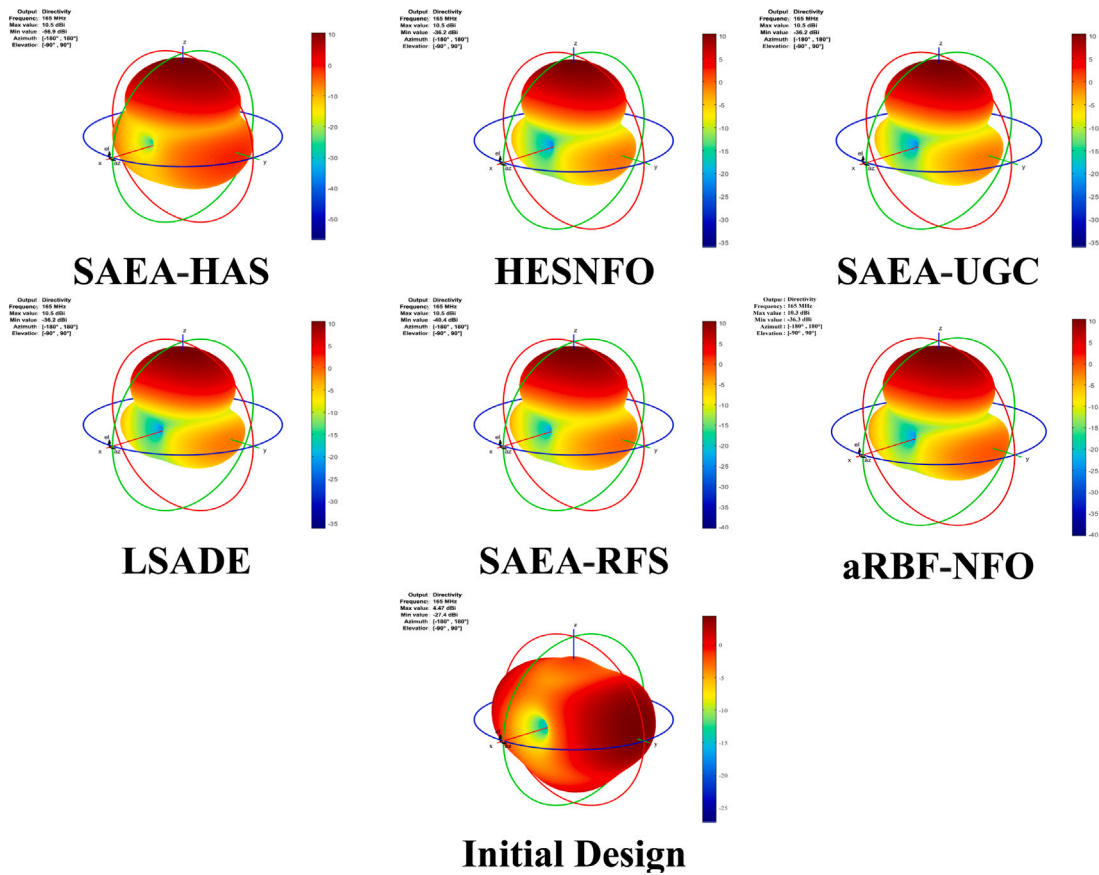


Fig. 9. The best radiation patterns of the Yagi-Uda antenna design problem obtained by SAEA-HAS and compared SAEAs.

It can be observed from Tables 5 to 7 that SAEA-HAS can provide better overall optimization performances in the 12 test problems than the other five SAEAs. SAEA-HAS and LSADE have similar convergence performance on the multi-modal test functions with low and medium dimensions. In addition, it is worth noting that SAEA-HAS can maintain good performance in obtaining better optimization results when the dimension of test problems increases.

4.7. Computational costs analysis

The total computation time of different SAEAs on all the test problems under different dimensions ($D = 10, 30, 50, 100$) is shown in Fig. 6. The computational time of each SAEA is computed by the *tic* and *toc* functions in MATLAB. As shown in Fig. 6, LSADE and SAEA-HAS have smaller computational costs than the other four algorithms on the test problems with 10 dimensions. Since SAEA-UGC and HESNFO include ensembles of surrogates in the construction process, the computational cost of these two algorithms is higher than that of the other four SAEAs. As the dimension increases, the computational costs of SAEA-UGC and HESNFO increase dramatically. SAEA-HAS exhibits well computational efficiency on medium dimensional test problems ($D = 30, 50$). In high-dimensional test problems, the computational efficiency of SAEA-RFS is higher than that of the other five SAEAs, and the computational costs of SAEA-HAS and aRBF-NFO are similar on test problems with 100 dimensions.

4.8. Application to Yagi-Uda antenna optimization problem

Geometry parameters significantly influence the radiation patterns of antennas; an optimal set of shape parameters is crucial for the design of antennas. The Yagi-Uda antenna is a radiating structure widely applied in various commercial fields. In this example, the above six

SAEAs are employed to optimize the structure of the Yagi-Uda antenna. The geometry of the Yagi-Uda antenna in Fig. 7 includes 10 design variables, namely the length of the reflector x_1 , lengths of the four directors x_2, x_3, x_4, x_5 , the reflector spacing x_6 and the four director spacings x_7, x_8, x_9, x_{10} . The initial design values of the Yagi-Uda antenna and the search ranges of different design variables are provided in Table 8, λ represents the wavelength. All the parameters in the center of the VHF band are the same as in Yu, Liang, Zhao et al. (2022). The optimization objective function of this design problem is to obtain a considerable value in the 90-degree direction, a smaller value in the 270-degree direction and a larger maximum power value between the elevation beam width-angle boundaries.

The Antenna Toolbox in MATLAB 2018b is employed to analyze the objective value. The experimental settings of the six SAEAs are the same as those introduced in Section 4.1. Each algorithm performs 20 times independently to avoid randomness.

Table 9 and Fig. 8 show the average optimization results of the six algorithms on the Yagi-Uda antenna design problem. The results in Table 9 and Fig. 8 indicate that SAEA-HAS has better optimization results and convergence ability than the other five SAEAs on the Yagi-Uda antenna design problem. The best-optimized radiation patterns of the Yagi-Uda antenna obtained by the algorithms and the radiation pattern of the initial design are shown in Fig. 9. Apparently, the initial design of the antenna cannot achieve a high directivity in the preferred direction. SAEA-HAS obtained the best radiation pattern and average objective values. The optimal design of SAEA-HAS has a large improvement in the radiation pattern. The optimized Yagi-Uda antenna obtained by SAEA-HAS achieves a forward directivity of 10.5 dBi. The front-to-back ratio is 67.4 dB, which is also part of the optimizer's maximization quantity.

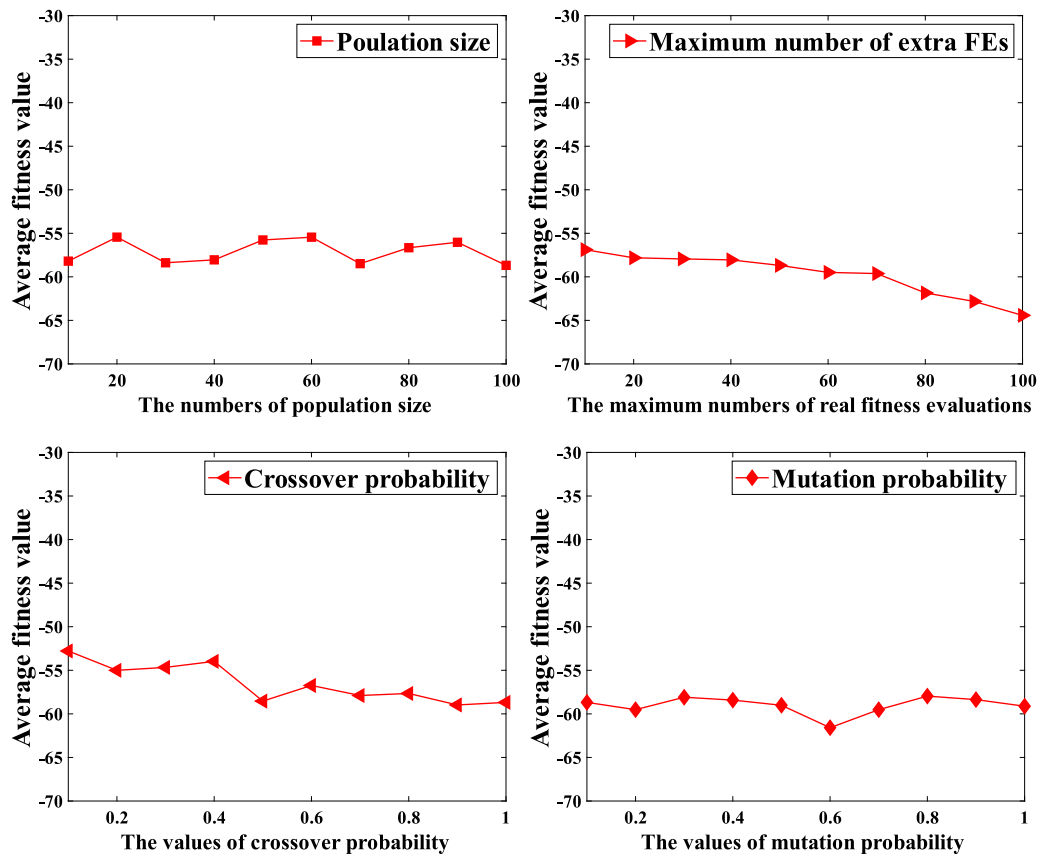


Fig. 10. Sensitivity analysis of parameters in SAEA-HAS to optimization results of Yagi-Uda design problem.

Table 9
Optimization results of different SAEAs on the Yagi-Uda antenna design problem.

Problem	Metric	SAEA-HAS	HESNFO	SAEA-UGC	LSADE	SAEA-RFS	aRBF-NFO
Yagi-Uda antenna design	Best	-7.788E+01	-5.710E+01	-5.710E+01	-5.710E+01	-7.147E+01	-6.316E+01
	Mean	-5.868E+01	-4.704E+01	-4.676E+01	-4.676E+01	-5.018E+01	-5.558E+01
	Std.	±6.961E+00	±2.602E+00	±2.434E+00	±2.434E+00	±7.095E+00	±5.595E+00
+ / ≈ / -		NA	+	+	+	+	+

Table 10
Ranges of the four parameters.

Parameter	Default value	Range
N_p	100	[10, 100]
N_{mf}	50	[10, 100]
p_c	1	[0.1, 1]
p_m	0.1	[0.1, 1]

4.9. Sensitivity analysis of parameters in SAEA-HAS

In this section, take the Yagi-Uda antenna optimization problem as an example, we have tested the sensitivity of the parameters that influence the optimization search process in SAEA-HAS, including population size N_p , maximum number of extra fitness evaluations N_{mf} , crossover and mutation probabilities p_c, p_m . When studying a certain parameter, the settings of the other three parameters are kept consistent with those in Section 4.8. The intervals of these four parameters are shown in Table 10, and ten points are uniformly taken for each parameter in the interval to study the sensitivity of the parameter on the optimization result. The SAEA-HAS performs independently 20 times in each experiment.

From Fig. 10, we can see that N_{mf} has the most significant influence on the convergence of the entire optimization result. With the increase

of N_{mf} , the convergence of the optimization results of the algorithm is better, indicating that more real fitness evaluations in the online SAEA can effectively improve the performance of the algorithm. In addition, when the crossover probability is greater than 0.4, the convergence of the algorithm will be improved to a certain extent. The population size and the mutation probability have no great influence on the convergence of the proposed algorithm. As for the mutation probability, when its value is 0.6, the convergence of the algorithm is relatively high.

5. Conclusion

To inherit the advantages of cut-HDMR modeling and bridge the gap between cut-HDMR and online SAEAs, this paper developed a surrogate-assisted evolutionary algorithm with the hierarchical surrogate technique and adaptive infill strategy (SAEA-HAS). Inspired by the cut-HDMR modeling, we developed a novel composite surrogate model constructed by the first-order cut-HDMR model and an error value-based surrogate model. An internal contrastive analysis method is applied to build the hierarchical surrogate model. Then an adaptive infill strategy is proposed to update the HSM during optimization and balance the exploration and exploitation of the surrogate-assisted evolutionary search. The effectiveness of SAEA-HAS is verified by twelve

Table A.1
The details of benchmark test problems.

Function	Characteristics	Mathematical formulation	Range
Ellipsoid	Uni-modal, Bowl-shaped	$f(x) = \sum_{i=1}^D ix_i^2$	$x_i \in [-5.12/2, 5.12]$
Rosenbrock	Uni-modal, Valley-shaped	$f(x) = \sum_{i=1}^{D-1} [100(x_{i+1} - x_i^2)^2 + (x_i - 1)^2]$	$x_i \in [-5, 10]$
Rotated Hyper-Ellipsoid	Uni-modal, Bowl-shaped	$f(x) = \sum_{i=1}^D \sum_{j=1}^i x_j^2$	$x_i \in [-65.536/2, 65.536]$
Trid	Uni-modal, Bowl-shaped	$f(x) = \sum_{i=1}^D (x_i - 1)^2 - \sum_{i=2}^D x_i x_{i-1}$	$x_i \in [-36/2, 36]$
Dixon-Price	Uni-modal, Valley-shaped	$f(x) = (x_1 - 1)^2 + \sum_{i=2}^D i(2x_i^2 - x_{i-1})^2$	$x_i \in [-10/2, 10]$
Ackley	Multi-modal, Many local minima	$f(x) = -20 \exp(-0.2 \sqrt{\frac{1}{D} \sum_{i=1}^D x_i^2}) - \exp(\frac{1}{D} \sum_{i=1}^D \cos(2\pi x_i)) + 20 + \exp(1)$	$x_i \in [-32.768/2, 32.768]$
Griewank	Multi-modal, Many local minima	$f(x) = \sum_{i=1}^D \frac{x_i^2}{4000} - \prod_{i=1}^D \cos(\frac{x_i}{\sqrt{i}}) + 1$	$x_i \in [-600/2, 600]$
Rastrigin	Multi-modal, Many local minima	$f(x) = 10D + \sum_{i=1}^D [x_i^2 - 10 \cos(2\pi x_i)]$	$x_i \in [-5.12/2, 5.12]$
Styblinski-Tang	Multi-modal, Many local minima	$f(x) = \frac{1}{2} \sum_{i=1}^D (x_i^4 - 16x_i^2 + 5x_i)$	$x_i \in [-5/2, 5]$
Shifted Rosenbrock	Shifted, Valley-shaped	$f(x) = \sum_{i=1}^{D-1} [100(z_{i+1} - z_i^2)^2 + (z_i - 1)^2] + f_{bias1}, z = x - o + 1$	$x_i \in [-100, 100]$
Shifted Rotated Griewank	Shifted, Rotated	$f(x) = \sum_{i=1}^D \frac{z_i^2}{4000} - \prod_{i=1}^D \cos(\frac{z_i}{\sqrt{i}}) + 1 + f_{bias2}, z = (x - o) * M$	$x_i \in [0, 600]$
Shifted Rastrigin	Shifted, Many local minima	$f(x) = \sum_{i=1}^D [z_i^2 - 10 \cos(2\pi z_i) + 10] + f_{bias3}, z = x - o$	$x_i \in [-5, 5]$

benchmark test problems and a Yagi-Uda antenna optimization problem that requires expensive simulations. We choose five SAEAs for comparison. Based on the experimental results, the following conclusions can be drawn:

- In most test problems (7 out of 9), the global prediction accuracy of HSM is much higher than that of the stand-alone RBF model under different dimensions (10, 30, 50, 100), indicating that the proposed HSM has good global prediction accuracy on both uni-modal and multi-modal problems. The contrastive analysis can effectively improve the robustness of HSM.
- SAEA-HAS with AIS shows better performance than that of SAEA-HAS with only performance-based fill criteria. AIS can improve the convergence performance of the proposed SAEA-HAS and enhance the exploration to exploitation of the surrogate-assisted evolutionary search. In addition, when the difference between the maximum function value and the minimum function value in the database increases, the AIS strategy will increase the mutation range, thereby adaptively improving the exploration ability of SAEA-HAS.
- According to the Friedman test results, SAEA-HAS has better overall performance than the other five SAEAs on low-dimensional test problems. The test results show that SAEA-HAS has better robustness and convergence ability on low-dimensional test problems than the other five SAEAs. Since SAEA-UGC and HESNFO include ensembles of surrogates in the construction process, the computational cost of these two algorithms is higher than that of the other four SAEAs.
- SAEA-HAS and LSADE show similar performance on multi-modal functions with medium and low dimensions. SAEA-HAS can provide better overall optimization performances in the high dimensional test problems than the compared SAEAs.
- SAEA-HAS has better optimization results and convergence ability than the other five SAEAs on the Yagi-Uda antenna design problem. SAEA-HAS obtained the best radiation patterns and average objective values. The optimized design of SAEA-HAS shows a significant improvement in the radiation pattern.

The experimental results in this work show that SAEA-HAS has better overall performance in the test problems, validating the effectiveness of the proposed SAEA. SAEA-HAS is expected to be widely applied in real-world optimization problems.

CRedit authorship contribution statement

Hao Chen: Conceptualization, Methodology, Visualization, Software, Writing – original draft, Writing – review & editing. **Weikun Li:** Validation, Data curation, Investigation. **Weicheng Cui:** Writing – review & editing.

Declaration of competing interest

The authors declare that they have no known competing financial interests or personal relationships that will influence the work reported in this paper.

Data availability

Data will be made available on request

Acknowledgments

This research was supported by Guangdong Key R&D Program of 2021 Ocean Six Industrial project No. 2021-45

Appendix. The details of benchmark test problems

See [Table A.1](#)

References

Andrés-Pérez, E., González-Juarez, D., Martin, M., Iuliano, E., Cinquegrana, D., Carrier, G., et al. (2019). Garteur ad/ag-52: Surrogate-based global optimization methods in preliminary aerodynamic design. In *Evolutionary and deterministic methods for design optimization and control with applications to industrial and societal problems* (pp. 195–210). Springer.

- Bi, Y., Xue, B., & Zhang, M. (2021). Genetic programming with image-related operators and a flexible program structure for feature learning in image classification. *IEEE Transactions on Evolutionary Computation*, 25, 87–101. <http://dx.doi.org/10.1109/TEVC.2020.3002229>.
- Box, G. E., Hunter, W. H., Hunter, S., et al. (1978). Vol. 664, *Statistics for experimenters: an introduction to design, data analysis and model building*. New York: John Wiley and sons.
- Cai, X., Gao, L., & Li, X. (2019). Efficient generalized surrogate-assisted evolutionary algorithm for high-dimensional expensive problems. *IEEE Transactions on Evolutionary Computation*, 24, 365–379.
- Chen, H., Li, W., Cui, W., & Liu, Q. (2022). A pointwise ensemble of surrogates with adaptive function and heuristic formulation. *Structural and Multidisciplinary Optimization*, 65, 1–23.
- Chen, H., Li, W., Cui, W., Yang, P., & Chen, L. (2021). Multi-objective multidisciplinary design optimization of a robotic fish system. *Journal of Marine Science and Engineering*, 9, 478.
- Chen, H., Li, W., Cui, W., et al. (2020). Disruption-based multiobjective equilibrium optimization algorithm. *Computational Intelligence and Neuroscience*, (2020).
- Chen, L., Wang, H., Ye, F., & Hu, W. (2019). Comparative study of hdmrs and other popular metamodeling techniques for high dimensional problems. *Structural and Multidisciplinary Optimization*.
- Chen, D.-R., Wu, Q., Ying, Y., & Zhou, D.-X. (2004). Support vector machine soft margin classifiers: error analysis. *Journal of Machine Learning Research*, 5, 1143–1175.
- Chugh, T., Chakraborti, N., Sindhya, K., & Jin, Y. (2017). A data-driven surrogate-assisted evolutionary algorithm applied to a many-objective blast furnace optimization problem. *Materials and Manufacturing Processes*, 32, 1172–1178.
- Cristianini, N., Shawe-Taylor, J., et al. (2000). *An introduction to support vector machines and other kernel-based learning methods*. Cambridge University Press.
- Cui, M., Li, L., Zhou, M., & Abusorrah, A. (2022). Surrogate-assisted autoencoder-embedded evolutionary optimization algorithm to solve high-dimensional expensive problems. *IEEE Transactions on Evolutionary Computation*, 26, 676–689. <http://dx.doi.org/10.1109/TEVC.2021.3113923>.
- Emmerich, M. T., Giannakoglou, K. C., & Naujoks, B. (2006). Single-and multiobjective evolutionary optimization assisted by gaussian random field metamodels. *IEEE Transactions on Evolutionary Computation*, 10, 421–439.
- Farzaneh, M., & Mahdian Toroghi, R. (2019). Music generation using an interactive evolutionary algorithm. In *Mediterranean conference on pattern recognition and artificial intelligence* (pp. 207–217). Springer.
- Friedman, J. H. (1991). Multivariate adaptive regression splines. *The Annals of Statistics*, 19, 1–67.
- Fu, G., Sun, C., Tan, Y., Zhang, G., & Jin, Y. (2020). A surrogate-assisted evolutionary algorithm with random feature selection for large-scale expensive problems. In *International conference on parallel problem solving from nature* (pp. 125–139). Springer.
- Gao, R., Wang, H., Yu, M., & Yue, Z. (2022). One parameter estimation-based approximation-free global adaptive control of strict-feedback nonlinear systems. *International Journal of Control, Automation and Systems*, 20, 1943–1950.
- Goel, T., Haftka, R. T., Shyy, W., & Queipo, N. V. (2007). Ensemble of surrogates. *Structural and Multidisciplinary Optimization*, 33, 199–216.
- Guo, D., Chai, T., Ding, J., & Jin, Y. (2016). Small data driven evolutionary multi-objective optimization of fused magnesium furnaces. In *2016 IEEE symposium series on computational intelligence* (pp. 1–8). IEEE.
- Hardy, R. L. (1971). Multiquadric equations of topography and other irregular surfaces. *Journal of Geophysical Research*, 76, 1905–1915.
- Hassoun, M. H., et al. (1995). *Fundamentals of artificial neural networks*. MIT Press.
- Hong, L., Cui, W., & Chen, H. (2021). A novel multi-robot task allocation model in marine plastics cleaning based on replicator dynamics. *Journal of Marine Science and Engineering*, 9, 879.
- Huang, P., & Wang, H. (2021). Comparative empirical study on constraint handling in offline data-driven evolutionary optimization. *Applied Soft Computing*, 110, Article 107603.
- Huang, P., Wang, H., & Jin, Y. (2021). Offline data-driven evolutionary optimization based on tri-training. *Swarm and Evolutionary Computation*, 60, Article 100800.
- Huang, P., Wang, H., & Ma, W. (2019). Stochastic ranking for offline data-driven evolutionary optimization using radial basis function networks with multiple kernels. In *2019 IEEE symposium series on computational intelligence* (pp. 2050–2057). IEEE.
- Jiang, B., Yang, J., Wang, X., Miao, S., & Bai, X. (2021). Optimization of pumps as turbines blades based on svm-hdmr model and pso algorithm. *Advances in Mechanical Engineering*, 13, 168781402111034364.
- Jin, Y., Olhofer, M., Sendhoff, B., et al. (2000). On evolutionary optimization with approximate fitness functions. In *Gecco* (pp. 786–793).
- Jin, Y., Wang, H., Chugh, T., Guo, D., & Miettinen, K. (2019). Data-driven evolutionary optimization: An overview and case studies. *IEEE Transactions on Evolutionary Computation*, 23, 442–458. <http://dx.doi.org/10.1109/TEVC.2018.2869001>.
- Kudela, J., & Matousek, R. (2023). Combining lipschitz and rbf surrogate models for high-dimensional computationally expensive problems. *Information Sciences*, 619, 457–477.
- Lan, W., Ye, Z., Ruan, P., Liu, J., Yang, P., & Yao, X. (2022). Region-focused memetic algorithms with smart initialization for real-world large-scale waste collection problems. *IEEE Transactions on Evolutionary Computation*, 26, 704–718. <http://dx.doi.org/10.1109/TEVC.2021.3123960>.
- Li, F., Cai, X., & Gao, L. (2019). Ensemble of surrogates assisted particle swarm optimization of medium scale expensive problems. *Applied Soft Computing*, 74, 291–305.
- Li, W. K., Chen, H., Cui, W. C., Song, C. H., & Chen, L. K. (2022). Multi-objective evolutionary design of central pattern generator network for biomimetic robotic fish. *Complex & Intelligent Systems*, 9, 1–21.
- Li, F., Gao, L., Garg, A., Shen, W., & Huang, S. (2021). Two infill criteria driven surrogate-assisted multi-objective evolutionary algorithms for computationally expensive problems with medium dimensions. *Swarm and Evolutionary Computation*, 60, Article 100774.
- Li, F., Gao, L., Garg, A., Shen, W., & Huang, S. (2021a). Two infill criteria driven surrogate-assisted multi-objective evolutionary algorithms for computationally expensive problems with medium dimensions. *Swarm and Evolutionary Computation*, 60, Article 100774. <http://dx.doi.org/10.1016/j.swevo.2020.100774>, <https://www.sciencedirect.com/science/article/pii/S2210650220304272>.
- Li, G., Hu, J., Wang, S.-W., Georgopoulos, P. G., Schoendorf, J., & Rabitz, H. (2006). Random sampling-high dimensional model representation (rs-hdmr) and orthogonality of its different order component functions. *The Journal of Physical Chemistry A*, 110, 2474–2485.
- Li, E., & Wang, H. (2016). An alternative adaptive differential evolutionary algorithm assisted by expected improvement criterion and cut-hdmr expansion and its application in time-based sheet forming design. *Advances in Engineering Software*, 97, 96–107.
- Li, E., Wang, H., & Ye, F. (2016). Two-level multi-surrogate assisted optimization method for high dimensional nonlinear problems. *Applied Soft Computing*, 46, 26–36.
- Li, J.-Y., Zhan, Z.-H., Wang, C., Jin, H., & Zhang, J. (2020). Boosting data-driven evolutionary algorithm with localized data generation. *IEEE Transactions on Evolutionary Computation*, 24, 923–937.
- Li, J.-Y., Zhan, Z.-H., Wang, H., & Zhang, J. (2020). Data-driven evolutionary algorithm with perturbation-based ensemble surrogates. *IEEE Transactions on Cybernetics*, 51, 3925–3937.
- Li, J.-Y., Zhan, Z.-H., & Zhang, J. (2022a). Evolutionary computation for expensive optimization: A survey. *Machine Intelligence Research*, 19, 3–23.
- Li, G., Zhang, Q., Sun, J., & Han, Z. (2019). Radial basis function assisted optimization method with batch infill sampling criterion for expensive optimization. In *2019 IEEE congress on evolutionary computation* (pp. 1664–1671). IEEE.
- Liu, B., Grout, V., & Nikolaeva, A. (2017). Efficient global optimization of actuator based on a surrogate model assisted hybrid algorithm. *IEEE Transactions on Industrial Electronics*, 65, 5712–5721.
- Liu, H., Hervas, J.-R., Ong, Y.-S., Cai, J., & Wang, Y. (2018). An adaptive rbf-hdmr modeling approach under limited computational budget. *Structural and Multidisciplinary Optimization*, 57, 1233–1250.
- Liu, Y., Liu, J., & Jin, Y. (2022). Surrogate-assisted multipopulation particle swarm optimizer for high-dimensional expensive optimization. *IEEE Transactions on Systems, Man, and Cybernetics: Systems*, 52, 4671–4684. <http://dx.doi.org/10.1109/TSMC.2021.3102298>.
- Liu, Y., Liu, J., & Tan, S. (2023). Decision space partition based surrogate-assisted evolutionary algorithm for expensive optimization. *Expert Systems with Applications*, 214, Article 119075.
- Liu, Q., Wu, X., Lin, Q., Ji, J., & Wong, K.-C. (2021). A novel surrogate-assisted evolutionary algorithm with an uncertainty grouping based infill criterion. *Swarm and Evolutionary Computation*, 60, Article 100787.
- Loh, W.-L. (1996). On latin hypercube sampling. *The Annals of Statistics*, 24, 2058–2080.
- Lu, X., Tang, K., & Yao, X. (2011). Classification-assisted differential evolution for computationally expensive problems. In *2011 IEEE congress of evolutionary computation* (pp. 1986–1993). IEEE.
- Mirjalili, S. (2019). Genetic algorithm. In *Evolutionary algorithms and neural networks* (pp. 43–55). Springer.
- Mukhopadhyay, T., Dey, T., Chowdhury, R., Chakraborti, A., & Adhikari, S. (2015). Optimum design of frp bridge deck: an efficient rs-hdmr based approach. *Structural and Multidisciplinary Optimization*, 52, 459–477.
- Qin, A. K., Huang, V. L., & Suganthan, P. N. (2009). Differential evolution algorithm with strategy adaptation for global numerical optimization. *IEEE Transactions on Evolutionary Computation*, 13, 398–417. <http://dx.doi.org/10.1109/TEVC.2008.927706>.
- Rabitz, H., & Aliş, Ö. F. (1999). General foundations of high-dimensional model representations. *Journal of Mathematical Chemistry*, 25, 197–233.
- Rabitz, H., Aliş, Ö. F., Shorter, J., & Shim, K. (1999). Efficient input-output model representations. *Computer Physics Communications*, 117, 11–20.
- Razavi, S., Tolson, B. A., & Burn, D. H. (2012). Review of surrogate modeling in water resources. *Water Resources Research*, 48.
- Sacks, J., Welch, W. J., Mitchell, T. J., & Wynn, H. P. (1989). Design and analysis of computer experiments. *Statistical Science*, 4, 409–423.
- Shan, S., & Wang, G. G. (2010). Survey of modeling and optimization strategies to solve high-dimensional design problems with computationally-expensive black-box functions. *Structural and Multidisciplinary Optimization*, 41, 219–241.

- Suganthan, P. N., Hansen, N., Liang, J. J., Deb, K., Chen, Y.-P., Auger, A., et al. (2005). Problem definitions and evaluation criteria for the cec 2005 special session on real-parameter optimization. *KanGAL Report 2005005*.
- Surjanovic, S., & Bingham, D. (2013). *Virtual library of simulation experiments: test functions and datasets*. Burnaby, BC, Canada: Simon Fraser University, (Accessed May, 13, 2015).
- Tong, H., Huang, C., Minku, L. L., & Yao, X. (2021). Surrogate models in evolutionary single-objective optimization: A new taxonomy and experimental study. *Information Sciences*, *562*, 414–437.
- Vt, S. E., & Shin, Y. C. (1994). Radial basis function neural network for approximation and estimation of nonlinear stochastic dynamic systems. *IEEE Transactions on Neural Networks*, *5*, 594–603.
- Wang, H., Feng, L., Jin, Y., & Doherty, J. (2021). Surrogate-assisted evolutionary multitasking for expensive minimax optimization in multiple scenarios. *IEEE Computational Intelligence Magazine*, *16*, 34–48.
- Wang, H., Jin, Y., & Doherty, J. (2017). Committee-based active learning for surrogate-assisted particle swarm optimization of expensive problems. *IEEE Transactions on Cybernetics*, *47*, 2664–2677.
- Wang, H., Jin, Y., & Jansen, J. O. (2016). Data-driven surrogate-assisted multiobjective evolutionary optimization of a trauma system. *IEEE Transactions on Evolutionary Computation*, *20*, 939–952.
- Wang, H., Jin, Y., Sun, C., & Doherty, J. (2018). Offline data-driven evolutionary optimization using selective surrogate ensembles. *IEEE Transactions on Evolutionary Computation*, *23*, 203–216.
- Wu, X., Peng, X., Chen, W., & Zhang, W. (2019). A developed surrogate-based optimization framework combining hdmr-based modeling technique and tbo algorithm for high-dimensional engineering problems. *Structural and Multidisciplinary Optimization*, *60*, 663–680.
- Wu, Z., Yu, M., & Liang, J. (2023). Parameter optimization of energy-efficient antenna system using period-based memetic algorithm. *Expert Systems with Applications*, *214*, Article 119131.
- Yu, M., Li, X., & Liang, J. (2020). A dynamic surrogate-assisted evolutionary algorithm framework for expensive structural optimization. *Structural and Multidisciplinary Optimization*, *61*, 711–729.
- Yu, M., Liang, J., Wu, Z., & Yang, Z. (2022). A twofold infill criterion-driven heterogeneous ensemble surrogate-assisted evolutionary algorithm for computationally expensive problems. *Knowledge-Based Systems*, *236*, Article 107747.
- Yu, M., Liang, J., Zhao, K., & Wu, Z. (2022). An arbf surrogate-assisted neighborhood field optimizer for expensive problems. *Swarm and Evolutionary Computation*, *68*, Article 100972.
- Yue, X., Zhang, J., Gong, W., Luo, M., & Duan, L. (2021). An adaptive pce-hdmr meta-modeling approach for high-dimensional problems. *Structural and Multidisciplinary Optimization*, *64*, 141–162.
- Zhang, N., Wang, P., Dong, H., & Li, T. (2020). Shape optimization for blended-wing-body underwater glider using an advanced multi-surrogate-based high-dimensional model representation method. *Engineering Optimization*, *52*, 2080–2099.
- Zhen, H., Gong, W., & Wang, L. (2022). Offline data-driven evolutionary optimization based on model selection. *Swarm and Evolutionary Computation*, *71*, Article 101080.
- Zhen, H., Gong, W., Wang, L., Ming, F., & Liao, Z. (2021). Two-stage data-driven evolutionary optimization for high-dimensional expensive problems. *IEEE Transactions on Cybernetics*, 1–12. <http://dx.doi.org/10.1109/TCYB.2021.3118783>.
- Zhou, Z., Ong, Y. S., Nair, P. B., Keane, A. J., & Lum, K. Y. (2006). Combining global and local surrogate models to accelerate evolutionary optimization. *IEEE Transactions on Systems, Man, and Cybernetics, Part C (Applications and Reviews)*, *37*, 66–76.
- Zhou, Z., Ong, Y. S., Nguyen, M. H., & Lim, D. (2005). A study on polynomial regression and gaussian process global surrogate model in hierarchical surrogate-assisted evolutionary algorithm. Vol. 3, In *2005 IEEE congress on evolutionary computation* (pp. 2832–2839). <http://dx.doi.org/10.1109/CEC.2005.1555050>.
- Ziegler, J., & Banzhaf, W. (2003). Decreasing the number of evaluations in evolutionary algorithms by using a meta-model of the fitness function. In *European conference on genetic programming* (pp. 264–275). Springer.